ENVIRONMENTAL PROTECTION AGENCY
OFFICE OF ENFORCEMENT

FIELD EVALUATION OF MOBILE LIDAR FOR THE MEASUREMENT OF SMOKE PLUME OPACITY

Project No. NEIC-TS-128

NATIONAL ENFORCEMENT INVESTIGATIONS CENTER
DENVER, COLORADO

February 1976

ENVIRONMENTAL PROTECTION AGENCY
OFFICE OF ENFORCEMENT
NATIONAL ENFORCEMENT INVESTIGATIONS CENTER
BUILDING 53, BOX 25227, DENVER FEDERAL CENTER
DENVER, COLORADO 80225

TO Mr. Lloyd Kostow
Region IX, S&A Division

DATE: August 12, 1976

FROM Remote Sensing Specialist

SUBJECT: Transmittal of the Lidar Report: Field Evaluation of Mobile Lidar for the Measurement of Smoke Plume Opacity

Attached are three copies of the subject report for your information. The main body of this report describes the lidar tests that were performed on the California ARB Smoke Generator, the Kaiser Permanente Facility and the Industrial Facilities at Lathrop, California. As an attachment to this report the technical report from the Stanford Research Institute is also included.

If you have any questions or comments, please do not hesitate to call me. I thank you for your assistance in setting up and making the contacts with the industrial facilities prior to the initiation of this study.

Arthur W. Dybdahl FTS 234-5306

Enclosures

ARB : Jeff Cook
BAY AREA : E. Brown

Contents

I. INTRODUCTION

The primary function of the National Enforcement Investigations Center (NEIC) of EPA is the collection of various types of environmental data for use as evidence in enforcement actions against polluters. Such data collection involves the use of a wide variety of techniques and instrumentation. Where possible, remote sensing techniques are used to complement traditional methods. Also, as new techniques are developed that are more reliable and accurate, NEIC employs them to ensure that the highest quality data are obtained.

With respect to emissions from stationary sources, plume opacity is one of the primary parameters monitored. Opacity is specifically limited by Federal, State or local regulations for practically all sources. The traditional method of monitoring plume opacity is visible emission observations (VEO's) performed by a trained human observer. An instrumental method involving the use of an optical transmissometer mounted in the stack or associated ductwork is increasingly being used for continuous monitoring of stack emissions. The two methods, however, are not directly comparable because they measure opacity at two different locations: one from the ducting leading to the stack and the other at the stack exit. The VEO's are also subject to interference by environmental conditions that sometimes limit their accuracy and frequently preclude their use.

Research performed by and for EPA has demonstrated that a remote sensing technique employing a mobile lidar* system is a reliable and accurate instrumental method of measuring plume opacity. The NEIC is procuring a mobile lidar system for use in collection of enforcement data.

---

* *Lidar, an acronym for Light Detection and Ranging, commonly refers to laser radar.*

In the development of technical specifications for the mobile lidar, other sources with similar equipment were investigated. The research performed at Research Triangle Park, N.C. (RTP) by EPA staff (1970 to 1974) pointed out the need for improvements in the data handling capability of the RTP lidar system. A mobile lidar system with a more sophisticated data processing capability and with the additional ability to track plumes of particulate emissions was contracted from the Stanford Research Institute (SRI), Menlo Park, California. NEIC conducted a limited-scope field study with the SRI lidar system to evaluate its performance under a variety of field and test conditions comparable to typical EPA enforcement data collection. Several calibration tests were conducted, including opacity measurements of emissions from a smoke generator used for certification of visible emission observers. Opacity was measured for visible emissions from three industrial plants during both daylight and darkness, and residual plumes were tracked.

The results of the SRI lidar study were used in the development of design and performance specificaitons for the NEIC lidar system. This report summarizes study conditions and the results of the study. Additional details are provided in the Attachment, the contractor's report, "*Lidar Applications for Smoke Plume Opacity Measurements, December 1975.*"

II. SUMMARY AND CONCLUSIONS

This field study was designed to evaluate the utility of various features of a mobile lidar (laser radar) system in the monitoring of smoke plume opacity and optical backscatter. The study was carried out with a contractor's lidar system in the San Francisco Bay area and in the San Joaquin Valley of California.

The following tests were performed with the lidar:

Clean Air Tests The lidar system electronics were calibrated including the linear and the logarithmic video amplifiers and the inverse-range-squared compensation circuitry.

Screen Tests An optical screen was used in conjunction with the lidar in order to evaluate the feasibility of using such a device as an opacity calibration target in the field. The use of screens is feasible; however, specular reflections from the wire grid and the degrading affects of field handling do present problems. Additional study is required to establish the practicality of screens for lidar calibration.

Smoke Generator Tests The lidar was used to interrogate (remotely test) the black and white smoke plumes emitted by a calibrated mobile smoke generator positioned 270 m (885 ft) away. The plumes from the generator stack were puffy which was manifested as a transient condition in the resultant plume opacity. The lidar easily documented the variations. However, the magnitude of the variations were not fully documented by the instack transmissometer because its response time was too slow to closely follow the excursions in opacity. Due to the low horizontal atmospheric visibility, this

test also afforded an evaluation of the lidar's receiver gating logic for controling incoming signal intensities resulting from the optical energy backscatter from the clean air in front of and behind the plume. Signal control for the backscattered energy from within the smoke plume was likewise evaluated.

Lidar Tests at Kaiser-Permanente The lidar observed visible stack emissions from cement kilns. The emissions contained water vapor which condensed near the stack opening. The lidar located the residual plume which contained only the particulate emissions after the condensed water aerosols had evaporated. This test also demonstrated the lidar's capability of measuring exit plume opacity even when a descending plume is in the lidar's line-of-sight to the stack exit. Both day and night tests were performed.

Lidar Tests at the Occidental Fertilizer Company and the Libby-Owens-Ford Company Observations of particulate emissions were made at night for opacity, dispersion and combination of small plumes. The lidar was an effective implement in the measurement and monitoring of these parameters.

These lidar tests revealed several very important features that need to be included in the mobile lidar system which EPA/NEIC is procuring.

1. The minimum effective aperture of the receiving telescope should be 20.3 cm (8 in) to aid in the detection of weak return signals from the clear air beyond a dense smoke plume.

2. The minimum output energy per pulse of the ruby laser should be 1.5 joules. Such a laser will provide sufficient peak power to yield a return (backscatter) signal for the clear air behind a dense or nearly opaque particulate plume, and thus

permit an accurate opacity determination. Calculation of opacity for a plume of greater than 80% opacity is not practicable with a lower output laser.

3. The maximum angular divergence of the laser beam should be 0.7 milliradians.

4. The ruby laser should have sufficient cooling capacity (for the head) to sustain a firing rate of a pulse every second in an ambient air temperature of at least 35°C (95°F). This will also be adequate for sustained lidar operation in hot summer weather.

5. The system must have a logarithmic video amplifier, in addition to a linear video amplifier, within the lidar electronics. The logarithmic amplifier will amplify weak signals such as the clear air return signal from behind a dense smoke plume, to a much greater level than the stronger signals from the clear air in front of the plume as well as from the plume itself. This will provide greater accuracy in measuring the opacity of dense plumes. This is especially true when measuring the opacity of a particulate plume within polluted areas (areas of heavy atmospheric burden). In this case, the "clear air" in front of a dense plume will have a much greater level of optical backscatter than when the air is reasonably clean (low pollution level). The return signal from the "clear air" behind the dense plume, in this case, will be orders of magnitude below that from in front of the plume and within the plume.

6. A gating logic capability within the lidar electronics is required to control backscatter return signal levels within the receiver, from in front of and within the plume. The

position of the gates (3 required) will be variable over the effective lidar range. This capability permits the detection, processing, and storage of the plume backscatter signal rather than blanking it out as is done in the EPA/Research Triangle Park lidar. There is valuable optical data in this plume backscatter signal which will be effectively used in the near future for plume tracking, the detection of the combining of plumes, plume dispersion and eventually mass emissions rates.

III. BACKGROUND

Smokestack emissions opacity has been an air pollution monitoring parameter in this country since the early 1900's. In recent years, the opacity of visible emissions has been determined by qualified visible emissions observers being used to gather the required data during daylight hours. The observers are tested every six months in accordance with Method 9. They must demonstrate the ability to assign opacity readings to black and white smoke plumes with an error not to exceed 15% opacity on any one reading and an average error not to exceed 7.5% in either smoke color category. For the most part they are limited to reading emissions during daylight hours with good sunlight.

The lidar is basically a laser radar used in the remote sensing of air pollution sources. In 1963, a lidar was successfully used to map laser backscattered echoes (red light) from turbidity in the upper atmosphere and to measure backscatter from the molecular constituents and haze in the lower atmosphere. Backscattered light is that fraction of light which is reflected back to the lidar from the aerosols present in the atmosphere. The lidar consisted of a ruby pulsed laser as an optical energy transmitter and a telescope/detector with the associated electronics as a lidar receiver. The electronics processed the lidar data and provided a usable output to the operator. It also contained a timing mechanism to measure the round trip time intervals for the back-scatter echoes from the time the pulse was transmitted from the laser to the time each echo was collected by the lidar receiver. This provided the range to each target.

In 1967, research was underway studying the use of lidar as a remote monitoring instrument for air pollution. Much has been done in

using the lidar as a remote monitor for particulates or aerosols being discharged from smokestacks and for the mapping of aerosols which occur in the lower atmosphere as a result of wind drift of smokestack emissions.

Today, tunable lasers are being used in lidar systems, in addition to a multitude of monofrequency lasers extending from the ultraviolet into the intermediate infrared.

The research and development of the monofrequency lidar has progressed to the point that it is ready for use in the EPA Enforcement Program to monitor the opacity of stationary source emissions. Initially, the lidar will be used in the Enforcement Program to remotely measure smokestack plume opacity. It is to that end that this field study was designed and carried out.

It is noteworthy to mention that lidars are under development for the detection and quantification of gaseous pollutants such as sulfur dioxide, ozone, and nitrogen dioxide. They should be available for field use within EPA in nearly two years.

IV. DESCRIPTION OF THE FIELD EVALUATION TESTS

The field evaluation tests for the lidar were designed to establish the performance characteristics of the lidar which includes calibration in a clear air medium and to establish a viable means of lidar field calibration which is easily reproduced from test site to test site. The tests performed with the lidar are outlined below.

Clean Air Tests

The lidar was fired in the horizontal position on a test range to obtain the necessary data to determine the state of calibration of the lidar system electronics. The output of the lidar was displayed on an oscilloscope. The curve on the scope displays a peak in the clear air backscatter signal intensity coincident with the convergence point of the lidar transmitter and receiver, i.e., they are looking at the same solid angle in space. This curve then falls off toward zero as 1/(range from lidar to scatterer)^2. The Mark IX lidar system electronics include a linear video amplifier, a logarithmic video amplifier (amplifies weak signals far more than the stronger lidar return signals), and an inverse-range-squared compensation circuit [1/(range from lidar to scatterer)^2]. The compensation circuit corrects the above mentioned fall-off curve for range, along the line-of-sight from the lidar, yielding a straight line on the oscilloscope parallel with the horizontal axis. This test serves as a performance check for the compensation circuit.

Screen Test

A means of lidar system calibration in the everyday field usage is a necessity being easy to employ with set-up and take-down time of less

than 5 minutes. This screen test must be consistently reproducible. Field calibration provides a quick check and verification of the accuracy with which the lidar can measure smokestack plume opacity. This capability is essential in employing the lidar in the enforcement mission.

The screen used in this test was approximately one square meter in size being constructed with a wooden frame and a fine wire mesh positioned over the frame. At the test range, the screen was set up nearly 150 m (500 ft) from the lidar (at a distance greater than the system convergence point where the laser and the telescope fields of view are coincident or completely overlap) permitting a field calibration referenced to the previously established opacity value of the screen. (Opacity is defined as one minus the optical transmittance of the screen, plume or any other target.)

This and many other lidar screen tests have shown that this calibration technique is not without problems which produce inaccuracies. Specular reflection has been isolated as a rather significant source of error when the lidar is measuring the opacity of a particular screen. Careful fabrication of the calibration screen may reduce the error to a negligible level. However, of major concern is the possible degrading effect field handling can impose on the optical properties of the screens.

The calibration test ultimately adopted for the EPA/NEIC lidar should yield a lidar calibration accuracy of 2 to 3% during both day and night hours. It is quite probable that nighttime calibration may be more effectual since optical scintillation induced by atmospheric turbulence along the line-of-sight of the lidar will be at a significantly lower level than that present during the daytime. Localized inhomogeneity in the air along the lidar line-of-sight is also an error source in attempting system calibration. Further study will be required to resolve these issues.

Smoke Generator Tests

These tests were performed in an open field during daylight hours using a mobile smoke generator provided and operated by the Air Resources Board, State of California, Sacramento, California. The smoke generator had a transmissometer that measured smoke plume opacity across its stack which was 4.6 m (15 ft) high. Black and white smoke plumes, generated with known opacities as monitored by the transmissometer, were interrogated (remotely tested) by light pulses from the lidar. The lidar was positioned 270 m (885 ft) from the smoke generator with the wind blowing nearly perpendicular to its line-of-sight at 8 to 16 km (5 to 10 mph). The horizontal visibility was less than 2 km at the test site.

The smoke generator emitted black or white smoke plumes over the range of 20 to 100% opacity. The opacity values were varied in 5 or 10% increments with each opacity value or level being interrogated with approximately 10 lidar pulses. The smoke plumes from the generator were not uniform but displayed a puffing characteristic. The wind also had an affect upon the rise (height above stack) of the plume. The lidar was aimed immediately above the opening of the generator stack to keep the lidar beam completely within the plume.

The technical details of these tests are documented in Section IV of the Attachment. The correlation values of smoke generator opacity (transmissometer) and lidar measured opacity for white smoke, are plotted in Figures 5 and 6 of the Attachment. In these plots the opacity values measured by the instack transmissometer were considered absolute or having no variation along the abscissa. Careful analysis of Figure 3, the smoke generator strip chart record, reveals that this indeed was not the case. A temporal variation in opacity was present in the smoke generator's plume as evidenced by the oscillations in the strip chart record. For the time interval given in Figure 5, Table 1 provides the

variation in smoke generator opacity for each nominal opacity value obtained from Figure 3.

Table 1†

Nominal Value of Opacity (%)	Range of Variation (%)	Difference in Opacity (%)
20	18-21	3
30	28-32	4
40	37-41	4
50		
60	59-62	3
70	68-71	3
80	78-81	3
90	89-91	2
100	99-100	1

† *Figure 3 Data, White Smoke, 1325-1400 PST, Dec. 3, 1975*

The spread ranges from 1% at the opaque end of the scale to 4% at the lower levels of opacity. In addition to the above, there was also the inaccuracy inherent to the smoke generator transmissometer in measuring the smoke opacity in the stack. Likewise, the response time of the transmissometer to the puffing or changes in plume particulate density is not of such a value to clearly document the full extent of the variations in opacity. The lidar measures plume opacity in a time interval of 30 nanoseconds (1 nanosecond = 10^{-9} seconds) while the response time due to signal integration in the instack transmissometer is in the order of 5 to 8 seconds. This time is more than 10^{8} times greater than that of the lidar. The lidar detects the instantaneous plume opacity, be it in either a dense area or in a less dense area of the varying smoke plume. The transmissometer averages the plume opacity values over the 5- to 8-second time period and is not capable of detecting the short lived peaks and valleys of the smoke plume opacity profile. Thus, the magnitude of the plume variations was not fully documented by the instack transmissometer.

All of these parameters outlined above are effective sources of error within the instack transmissometer and the effect is manifested in the divergence of the smoke generator data and the lidar data. Likewise, Table 2 depicts the variation in smoke generator opacity of the data presented in Figure 3 for the time interval given in Figure 6.

Table 2†

Nominal Value of Opacity (%)	Range of Variation (%)	Difference in Opacity (%)
20		
30	27-32	5
40	37-43	6
50	47-53	6
60	56-63	7
70	67-73	6
80	78-82	4
90	89-91	2
100	99-100	1

† *Figure 3 Data, White Smoke, 1415-1425 PST, Dec. 3, 1975*

The variation pattern is nearly the same as that described for the Figure 5 data. The variation pattern for the black smoke data contained in Figure 3 is provided in Tables 3 and 4.

Table 3†

Nominal Value of Opacity (%)	Range of Variation (%)	Difference in Opacity (%)
50	46-60	14
60	50-70	20
70	63-80	17
80	69-85	16
90	84-94	10
95	92-98	6

† *Figure 3 Data, Black Smoke, 1400 to 1410 PST, Dec. 3, 1975*

Table 4†

Nominal Value of Opacity (%)	Range of Variation (%)	Difference in Opacity (%)
20	18-23	5
30	26-34	8
40	37-42	5
50	45-54	9
60	51-66	15
70	63-75	12

† *Figure 3 Data, Black Smoke, 1435 to 1450 PST, Dec. 3, 1975*

The difference in opacity values about the respective nominal values for the black smoke displayed a variation pattern similar to that of white smoke. However, the magnitude of this difference was several times greater than that for white smoke. The black smoke plumes also appeared to be more turbulent or puffy than the white smoke plumes.

As was mentioned earlier in this report, the horizontal visibility in this location during the time of these tests, was less than 2 km. This became a significant factor in the smoke readings obtained by visible emission observers. The background sky was light gray due to the heavy atmospheric burden (air pollutants). The VEO readings for white smoke were consistently at least 20% lower than those obtained with the lidar and the smoke generator transmissometer. The black smoke presented a high color contrast against the background sky, and therefore greater accuracy was achieved with lidar/VEO variations of nominally 5 to 10%.

Due to the low horizontal atmospheric visibility, this test also afforded an evaluation of the lidar receiver gating logic for controlling incoming signal intensities resulting from optical energy backscatter from the clear air in front of, and behind the plume. Signal control for backscattered energy from within the plume was likewise evaluated.

Lidar Tests at Kaiser-Permanente

Both day and night tests were carried out with the lidar at the Kaiser-Permanente Cement and Gypsum Corporation, Cupertino, California, on Dec. 2, 1975. Three smoke plumes were interrogated with the lidar. The three stacks shown in Figure IV-1, were labeled #1 Stack, West Stack and East Stack. These stacks discharge emissions originating from cement kilns. Exhaust from #2 Kiln is discharged through the East Stack and the #5 Kiln through the West Stack. These stacks are 64 m (210 ft) high with 6.1 m (20 ft) exit diameters. The emissions from #1 Kiln pass through an electrostatic precipitator (esp) and are discharged through #1 Stack which is 38.1 m (125 ft) high with an exit diameter of 2.74 m (9 ft). Emissions from #6 Kiln were discharged through an electrostatic precipitator and out #6 Stack which is 30.5 m (100 ft) in height and has an exit diameter of 2.44 m (8 ft). This stack was not in operation at the time of this study. The remainder of the kilns, #3 and #4, discharge into two American Filter baghouses each having ten units. The baghouse emissions were not observed with the lidar.

The particulate plumes from these stacks drift a significant distance into the valley below [Fig. IV-2]. The stack emissions from the East and West Stack were photographed on October 29, 1975 near sunset during the preliminary test site visit.

The three plumes are known to contain a significant amount of water vapor which condenses near the exit of the stack. The water vapor would affect the VEO readings because water aerosols decrease light transmittance (increase plume opacity) just as particulates do. The aerosols also have a significant effect upon sunlight scatter as shown in Figures IV-3 and IV-4. In the former, the photograph was exposed from a hillside above the plant looking east while the sun was low in the west, with the valley terrain as a background. This arrangement would be in accordance with the viewing requirements of Method 9.

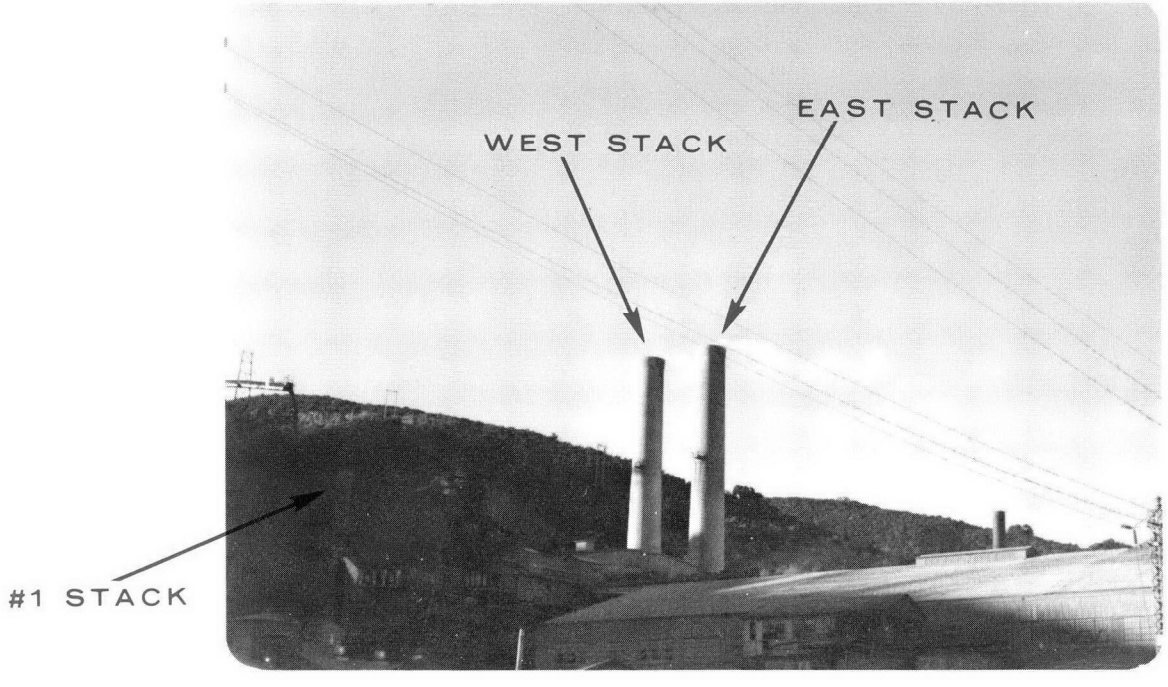

FIGURE IV-1 KAISER-PERMANENTE CEMENT CO. STACKS

PHOTOGRAPHED OCTOBER 29, 1975 NEAR SUNSET

FIGURE IV-2 KAISER-PERMANENTE CEMENT CO.

STACK EMISSIONS AND SUBSEQUENT DISPERSION

PHOTOGRAPHED OCTOBER 29, 1975 JUST AFTER SUNSET

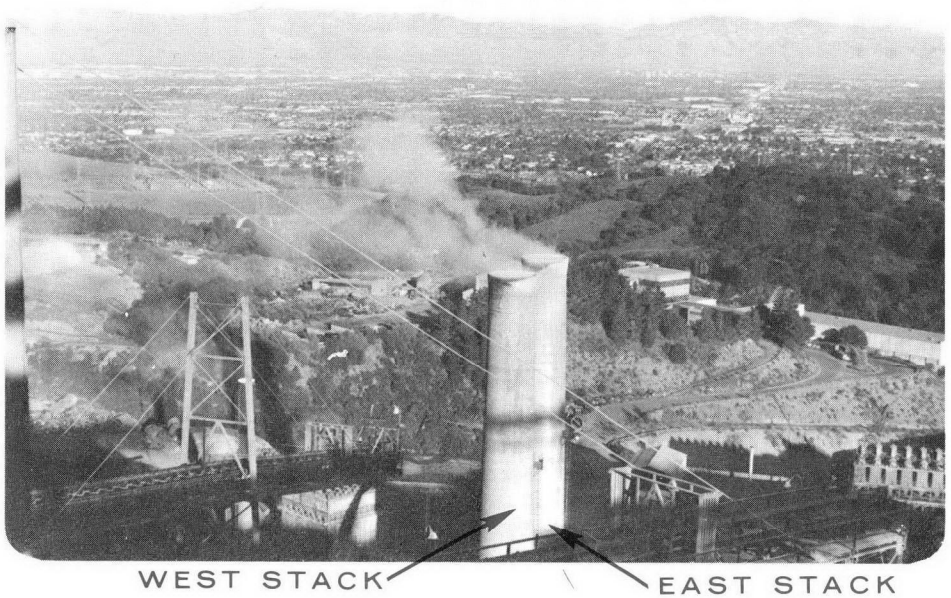

FIGURE IV-3 VIEW OF PARTICULATE PLUMES FROM THE EAST AND WEST STACKS LOOKING EAST WITH THE SUN LOW IN THE WEST (SUN LIGHT BACKSCATTERED OFF PLUME) PHOTOGRAPHED OCTOBER 29, 1975

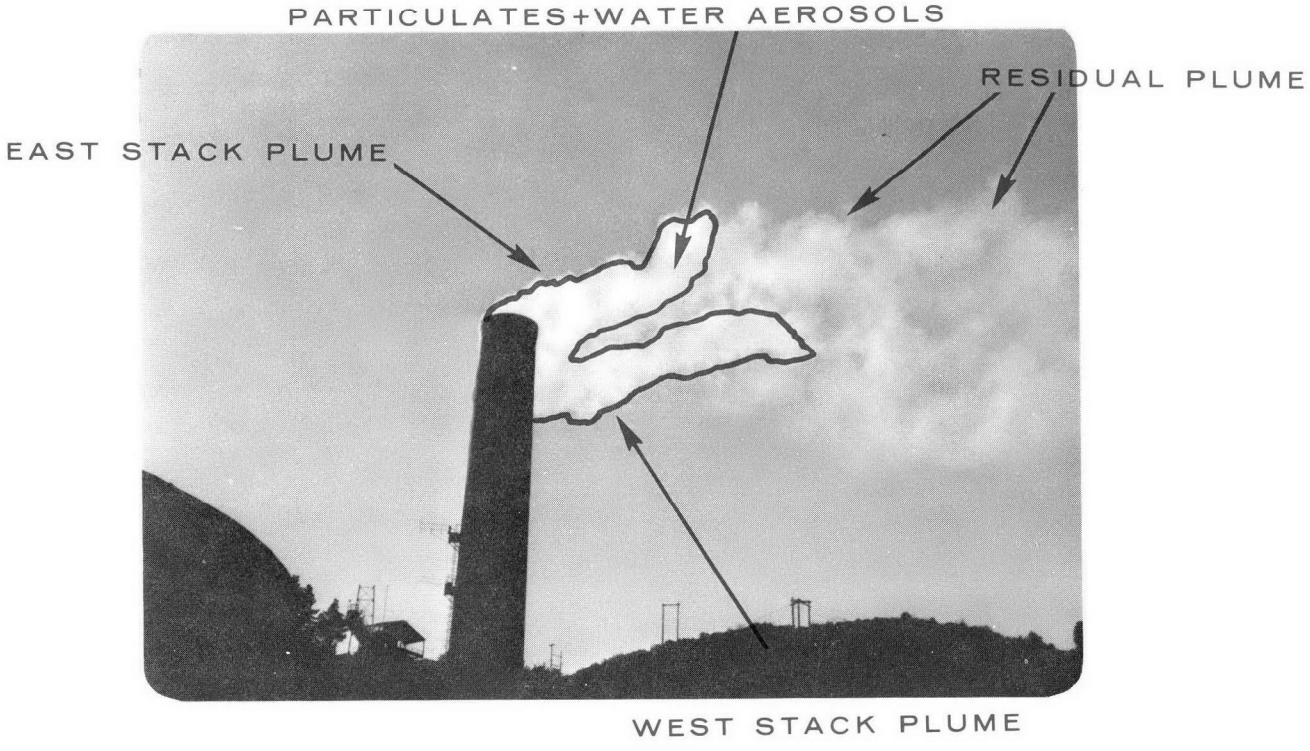

FIGURE IV-4 VIEW OF PARTICULATE PLUMES FROM THE EAST AND WEST STACKS LOOKING WEST WITH THE SUN LOW IN THE WEST (SUN LIGHT FORWARD-SCATTERED FROM PLUME) EAST AND WEST STACKS IN-LINE PHOTOGRAPHED ON OCTOBER 29, 1975

However, the line of demarcation cannot be clearly defined between the region of the plume containing particulates and condensed water aerosols, and the residual region of the plume where the condensed water microdroplets evaporated leaving only the particulates. This presents a major problem because the water aerosols are not pollutants but the particulates are so classified. Regulations only apply to the particulates as related to plume opacity. In Figure IV-4, the stacks were photographed looking west with the sun low in the west. The plumes from the east and west stacks appear much brighter and pronounced because the forward-scatter of sunlight by the particulates and water aerosols is far greater than solar backscatter [Fig. IV-3]. Also shown in this figure are the two regions of the plume mentioned above which were not discernible in Figure IV-3 (these two photographs were recorded only minutes apart).

The plumes from the East, West and #1 Stacks were interrogated with the lidar positioned south of the stacks. The line-of-sight was nearly perpendicular to the common-line of the East and West Stacks. The exit plume opacity of each stack was measured and was found to have the following ranges of opacity [Table 5]:

Table 5

KAISER SMOKESTACK EXIT PLUME OPACITY

Stack	Opacity Range (%)	Dominant Value (%)
East Stack	35-75	65
West Stack	20-75	50
#1 Stack	20	20

The plume was drifting in a southerly direction due to a northerly breeze present at the time of test. Many times during this study the smoke plumes would drift as a slowly dispersing entity to elevation levels below the exit height of the stacks and coincident with the

line-of-sight of the lidar and VEO (fumigating lapse condition). This occurrence completely precluded the smoke reading of the exit plume with the VEO's. However, the lidar is range-resolved; the range or distance between the lidar and the plume(s) and beyond the plumes is segmented into equal intervals or range cells usually on the order of 3 to 15 meters in length. Thus, the lidar can measure the exit plume opacity even with a descending plume condition, if there is at least one range cell between the descending plume condition, if there is at least one range cell between the descending plume and the exit plume. This condition is required in order to obtain a clear air return signal, which is needed from in front of and behind the exit plume for the opacity calculation [Chapter II, Attachment]. This is depicted in the lidar cross section [Fig. 10, Attachment] provided as (a)2. One can easily see the separation of the two plumes in the lower center of the photograph. There was ample clear air return range between the two plumes, permitting calculation of the opacity of the rear (exit) plume.

The oscilloscope photographs of Figure 10 [Attachment I] depict the two aforementioned sections or regions of a plume, namely, the plume of particulates and water aerosols, and the plume of only particulates. The white area in each photograph is the particulate/aerosol plume while the light gray/medium gray area is the residual plume, or the plume consisting of only particulates remaining after the water aerosols had evaporated. These lidar cross sections were made after sunset into the early evening.

Lidar Tests at Occidental Fertilizer Company and Libby-Owens-Ford (LOF) Company

After the smoke generator/lidar tests were completed in late afternoon on Dec. 3, 1975, the lidar was used to interrogate four stacks located within the Occidental and LOF facilities in Stockton (Lathrop),

California. These two facilities are adjacent to each other. One of the stacks was on the Occidental facility (Stack 1) while Stacks 2, 3 and 4 were on the LOF facility. From after sunset into darkness, over 120 lidar shots were made, measuring the opacity of the plumes from the four stacks and the azimuthal cross sections of the plumes from Stacks 2, 3, and 4 since they were in proximity to each other. The data for each stack plume is presented in Table 6.

Table 6

INDUSTRIAL SMOKESTACK OPACITY

Stack No.	Opacity Range (%)	Average Opacity (%)	No. of Lidar Shots
1	19-42	30	24
2	40-95	71	30
3	83-99	90	36
4	90-98	92	33

Stacks 1 and 2 displayed a rather large variation in opacity values. There was a puffing characteristic in the exit plumes. The exit plumes from Stacks 3 and 4 being larger in diameter than from Stacks 1 and 2 were much more consistent in opacity values. The California Air Resources Board (ARB) said during the tests that the plumes from Stacks 2, 3 and 4 contained condensed water aerosols characteristic of industrial process at LOF. The same characteristic observed in the Kaiser-Permanente facility is present in the azimuthal cross-sectional scan of Figure 12 of the Attachment. The white areas within the plume structure had an opacity of nearly 100% when the scan was performed, possibly consisted of both particulates and condensed water aerosols. The light/medium areas were the residual plume wherein the aerosols were not present due to evaporation.

The lidar azimuthal scan also depicts where the three individual plumes were combining, the direction of drift (to upper right), and the dispersion characteristics along the drift path.

The technical details of this test are given in Section VI of the Attachment.

ATTACHMENT

LIDAR APPLICATIONS FOR SMOKE PLUME OPACITY MEASUREMENTS

STANFORD RESEARCH INSTITUTE
MENLO PARK, CALIFORNIA

STANFORD RESEARCH INSTITUTE
Menlo Park, California 94025 • U.S.A.

Final Report *December 1975*

LIDAR APPLICATIONS FOR SMOKE PLUME OPACITY MEASUREMENTS

By: EDWARD E. UTHE

Prepared for:

NATIONAL ENFORCEMENT INVESTIGATIONS CENTER
OFFICE OF ENFORCEMENT
U.S. ENVIRONMENTAL PROTECTION AGENCY
DENVER, COLORADO
ATTENTION: A. DYBDAHL

EPA PURCHASE REQUISITION NO. TS-129

SRI Project No. 4723

Approved by:

R. T. H. COLLIS, *Director*
Atmospheric Sciences Laboratory

RAY L. LEADABRAND, *Executive Director*
Electronics and Radio Sciences Division

CONTENTS

I INTRODUCTION

The National Enforcement Investigations Center (NEIC), Office of Enforcement, U.S. Environmental Protection Agency, Denver, Colorado, contracted with Stanford Research Institute for remote sensing services to evaluate and demonstrate the application of lidar instrumentation for the collection of data in support of the enforcement monitoring program for air quality. Because of budget constraints, the field program was limited to three observational days, using the already existing capabilities of the SRI Mark IX Mobile Lidar System. This report presents the major results of this field investigation and of a limited data analysis effort.

II BACKGROUND AND METHOD OF APPROACH

SRI has pioneered the use of lidar in the remote observation of stack plume optical and physical densities and plume transport and diffusion characteristics. The first lidar measurements in the lower atmosphere were made by SRI in the summer of 1963. Approximately a year later, Dr. M.G.H. Ligda suggested a technique to remotely measure smoke plume densities by comparing the lidar returns from the clear air before and after the penetration of the plume by the laser energy. The plume opacity 0 (actually one minus the transmission at the lidar wavelength) is then given as:

$$0 = 1 - \sqrt{I/I_o}$$

where

I_o = backscatter signal before the plume return

I = backscatter signal after the plume return.

The plume opacity technique was shown feasible in a series of tests conducted for the Edison Electric Institute by Fernald and Collis (1965) and a mobile lidar system was designed by Evans (1967) for application of the technique. The system was constructed by General Electric for the Environmental Protection Agency (EPA) and has been extensively evaluated on EPA research programs (Cook, Bethke, and Conner, 1972).

A difficulty with the opacity technique is that the large plume return may saturate the sensitive photomultiplier detector and, because of the detector's relatively long recovery time, render accurate measurements of the far side clear-air backscatter impossible. The EPA lidar has been modified to overcome this difficulty by electronically gating

out the plume return. Another difficulty is the accurate observation of the clear air return from the far side of the plume for dense plumes because of the relatively low intensity signals that result. The approach taken by SRI is to use a video logarithmic amplifier that suppresses the large plume return while amplifying the less intense clear air returns. In addition, the receiver gain is electronically controlled in three steps. For the plume opacity measurement, the first step is adjusted to reduce the receiver gain out to the range of the plume. This first step prevents the "clear air" return originating from near the lidar from saturating the detector and log amplifier. The second gain reduction step is triggered at the end of the first step and further reduces receiver gain to prevent saturation by the plume return. The attenuation and range intervals of the gain reduction steps are adjustable so that both clear air and plume returns can be observed and evaluated. At the end of the second step, the receiver gain is turned on to full value so that clear air return may be observed at maximum receiver sensitivity. As shown in the following sections of this report, the log amplifier aids in the observation of the signal from beyond the plume.

Another approach to plume density measurement is to relate the backscatter from the plume to the plume density. In a series of experiments conducted by dispersing plume particulates (fly ash) of known size, shape, concentration, and refractive properties in a specially designed aerosol chamber--allowing unobstructed lidar observations of aerosols in realistic plume geometries--Uthe and Lapple (1972) were able to demonstrate that the plume return for a 700-nm wavelength lidar is well correlated with the plume <u>opacity</u> (one minus the transmission of light with wavelength dependance identical to that of the eye response), irregardless of the particle size. In addition, the plume return for a 1060-nm wavelength lidar is well correlated with plume <u>physical density</u> irregardless of particle size. The plume backscatter technique would

place fewer requirements on the lidar instrumentation than the clear air opacity technique.

Multiple lidar signatures recorded while the lidar scans in either evaluation or azimuth directions can be used to derive space and time variations of plume density distributions. These data can then be analyzed in terms of plume transport and diffusion characteristics as a function of local topography and meteorological conditions. Initially, the use of lidar in these roles relied on the handprocessing of lidar signatures (signal intensity recorded as a function of range) into two-dimensional isoscattering diagrams (Johnson, 1969). Later, the signatures were hand digitized and computer analyzed using polar-coordinate plotting routines (Johnson and Uthe, 1971). The computer processing of digital records also facilitated the correction of the plume cross sections for the attenuation effect and the computational inference of cross-plume integrated densities (Johnson and Uthe, 1971).

The video disk technique of recording and processing lidar signatures was introduced by SRI as an inexpensive means of electronically generating pictorial displays of aerosol structure from recorded lidar data (Allen and Evans, 1972). Johnson et al., (1973) used the video disk technique to investigate plume geometric properties in both urban and rural environments. While the technique gave a readily available means to view plume structure in both space and time, the disk records were not suitable for quantitative density evaluations because of bandwidth problems.

The rapid development of commercial high-speed digitizers, minicomputers, and digital display systems now make digital data processing capabilities generally available at relatively low cost. Recently, SRI has taken advantage of commercially available components to construct a digital real-time lidar data recording, processing, and display system

for its Mark IX mobile lidar facility (Uthe and Allen, 1975). The system provides much higher signal processing accuracy than the video disk technique and provides both real-time analysis and display of processed lidar data. The system has been applied to the remote observation of cirrus clouds and urban boundary layers but only recently has been applied to plume studies. A journal reprint describing the capabilities of the Mark IX digital system is reproduced in this report as Appendix A.

On 2 December 1975 the Mark IX lidar was operated at the Kaiser-Permanente cement plant located in Cupertino, California. The lidar was operated without the gain reduction steps. All data collected on this program were recorded on the digital system for both real-time and subsequent data analysis. Inspection of the results obtained at Permanente showed that the usefulness of the data obtained by the lidar without the gain reduction steps was limited to plume opacities of 0.7 or less.

On 3 December the lidar was operated near Stockton, California. The State of California Air Resources Board operated a calibrated smoke generator in support of the lidar tests. Plumes from 20 to 100 percent opacity were generated with both white and black smoke. Later, the lidar was used to observe plumes from Occidental and Libbey-Owens-Ford manufacturing plants. The logarithmic amplifier and gain reduction steps were used for all data collected on 3 December. In addition to the plume opacity measurements, the lidar was scanned in both elevation and azimuth angles to produce vertical and horizontal cross sections of plume structure.

On 4 December the lidar was operated at the Stanford Field Site to obtain clear air backscatter data for calibration of the log amplifier response function and to calibrate the receiver gain reduction steps. The results of these field observations are presented in the following sections of this report.

III LIDAR CALIBRATION TESTS

A receiver of large dynamic range is required to accurately observe backscatter from the clear air on the near and far side of the plume and from the plume particulates. Figure 1 presents the relationship between opacity and the near and far side clear air returns (signal difference in dB = 10 log I/I_o). For a plume of 90 percent opacity, a signal difference of 20 dB (or a factor of 0.01) must be resolved by the lidar receiver. In addition, the plume return may be as much as 30 dB above the near side clear air return. For these reasons, a video logarithmic amplifier and receiver gain reduction steps were thought necessary for observation of dense plumes.

The response of the Mark IX logarithmic receiver and gain reduction steps were calibrated by repeatedly firing the lidar into clear air while reducing the receiver gain in known steps by inserting neutral density filters in front of the detector. The Biomation 8100 digitizer settings during this calibration were:

Voltage setting = 0.2 V
Voltage offset = -.79
Delay setting = .04
Sampling rate = .01 μs

Biomation counts recorded at the same range were averaged for 10 laser firings. The results for various neutral density filters and receiver gain reduction steps are shown in Figure 2. These results show that the Biomation counts can be related to light input to the receiver by the value 0.2 dB/count up to a value of 70 counts--above which a non-linear response occurs. Since the noise level of the receiver was determined as -105 counts, the receiver has a linear logarithmic response over a

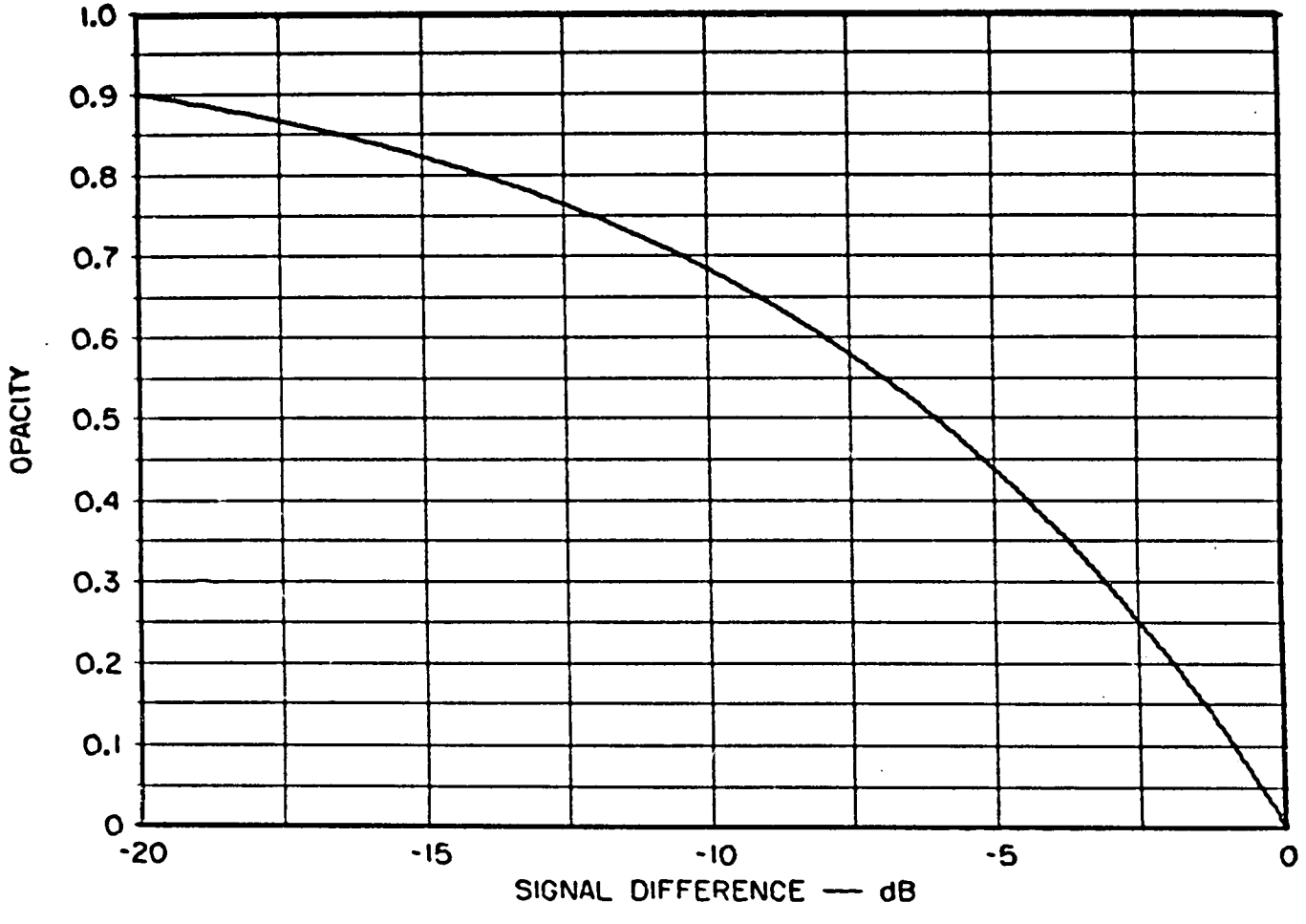

FIGURE 1 PLUME OPACITY AS A FUNCTION OF THE SIGNAL DIFFERENCE (in dB units) BETWEEN THE NEAR AND FAR SIDE CLEAR AIR RETURNS

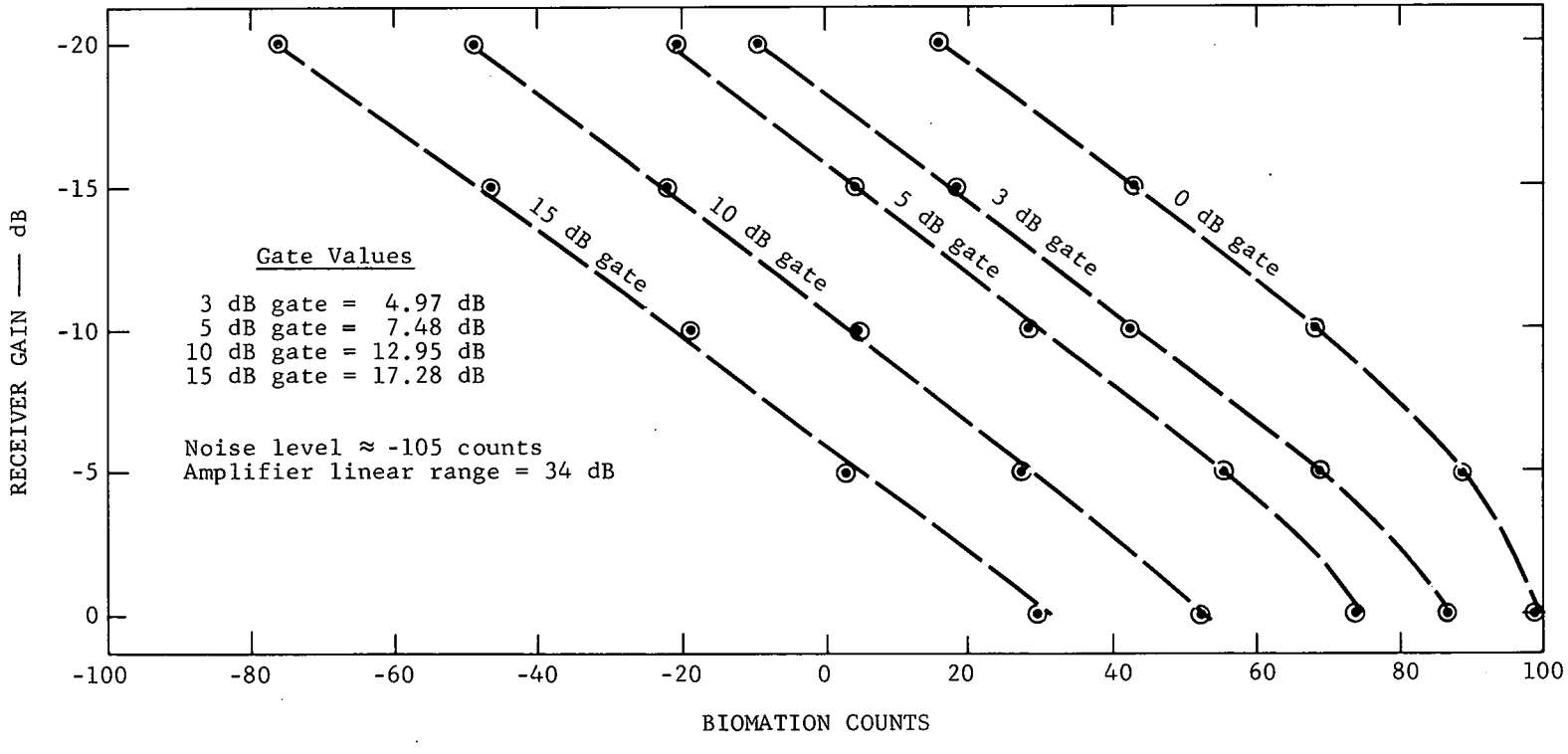

FIGURE 2 CLEAR AIR CALIBRATION OF LOG AMPLIFIER AND GAIN REDUCTION STEPS (4 December 1975)

range of 34 dB. From the calibration data presented in Figure 2, the gain reduction steps were determined as:

Step marked 3 dB = 4.97 dB
Step marked 5 dB = 7.48 dB
Step marked 10 dB = 12.95 dB
Step marked 15 dB = 17.28 dB

Since the Biomation has a count range of -256 to +256, the voltage resolution could be improved by adjusting Biomation settings; however, the resolution and dynamic range is satisfactory for the plume studies conducted under this program.

IV SMOKE GENERATOR TESTS

The State of California Air Resources Board operated a calibrated smoke generator in support of the lidar evaluation tests. Black and white plumes were generated with known opacities as measured by an across-the-stack transmissometer. Transmissometer records for the period of the lidar tests are shown in Figure 3.

The Mark IX lidar van was located 270 meters from the smoke generator and the lidar beam was aligned on the plume near the top of the generator stack. Approximately 10 backscatter signatures were recorded for each opacity setting. Typical backscatter signatures as recorded on tape and displayed on the digital monitor (see Appendix A) are shown in Figure 4. These signatures were digitally corrected for the inverse range squared dependence. Figure 5 presents a plot of the lidar observed opacities against the transmissometer opacities for the white smoke generated during the time period 1325-1400 PST. These data illustrate that the lidar technique produces values that are in general agreement with the transmissometer values over the range of 20 to 100 percent opacity. The scatter in the data are primarily a result of plume spreading and a resulting reduction in plume opacity downwind of the stack emission; the data of Figure 5 show that the lidar derived values are generally lower than the transmissometer values. Another major source of error can be introduced by differences in the backscatter properties of the clear air in front of and behind the plume. If the plume particulates increase the clear air backscatter in front of the plume relative to that from behind the plume, the lidar observed opacity will overestimate the true opacity. If the clear air behind the plume produces greater backscatter than the

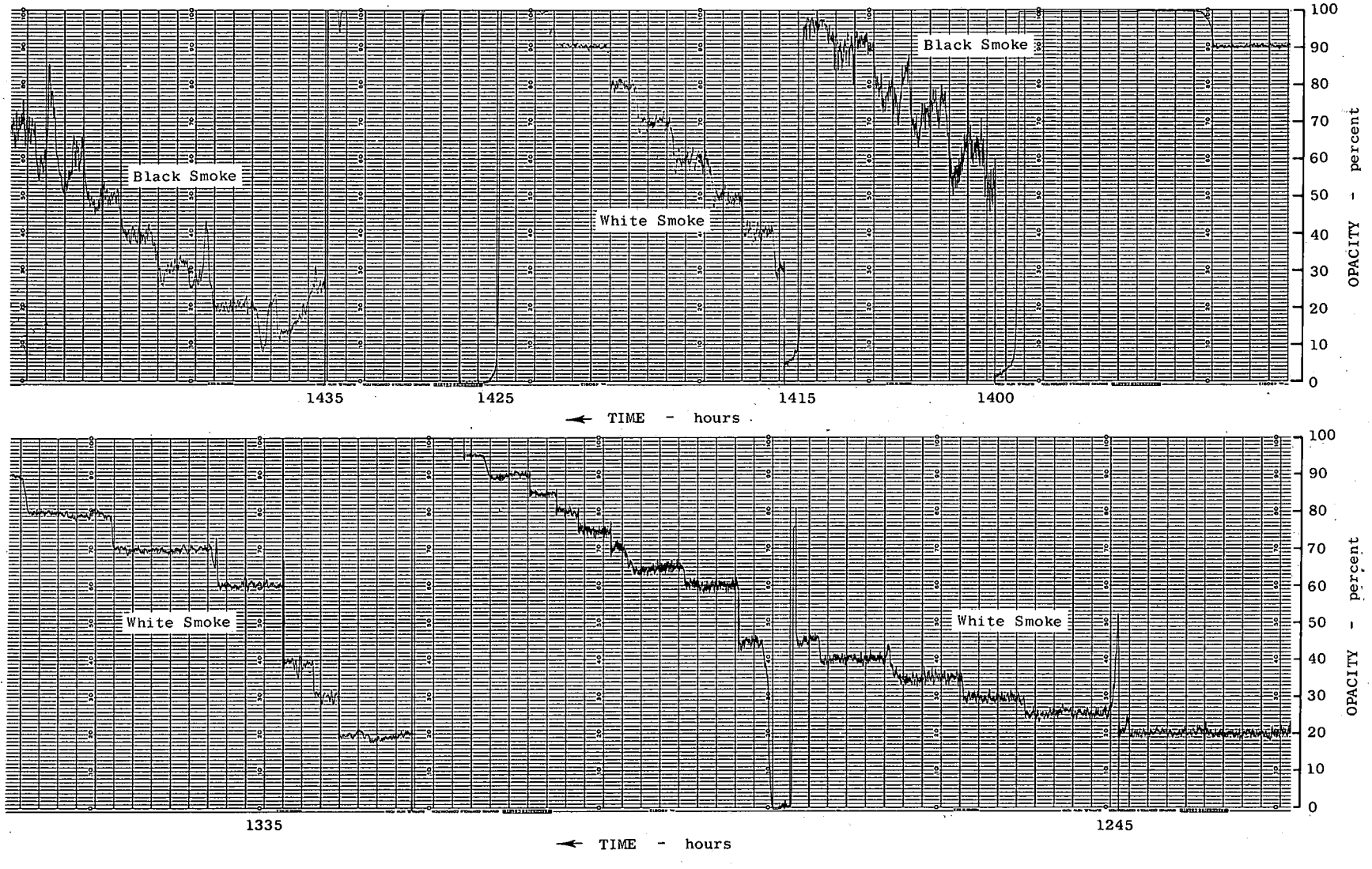

FIGURE 3 STRIP-CHART RECORD OF PLUME OPACITY AS MEASURED BY TRANSMISSOMETER

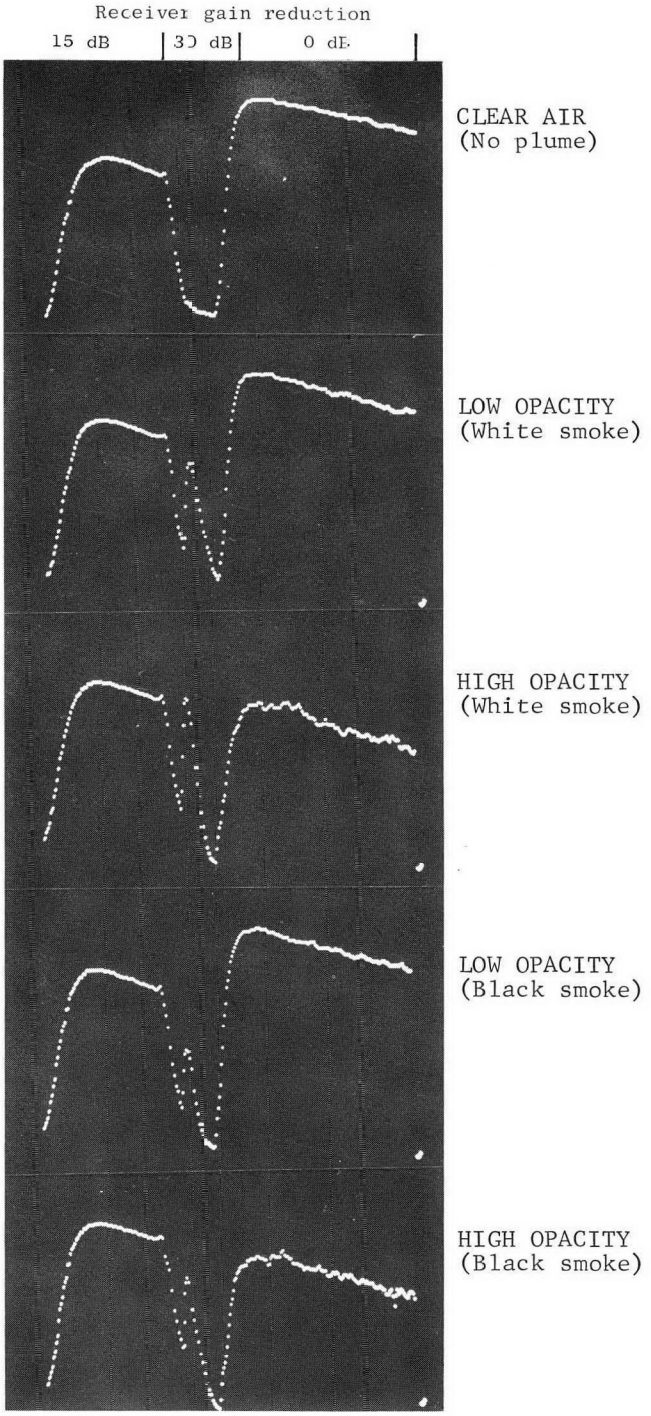

FIGURE 4 EXAMPLES OF LIDAR BACKSCATTER SIGNATURES OBSERVED ON DIGITAL SCREEN

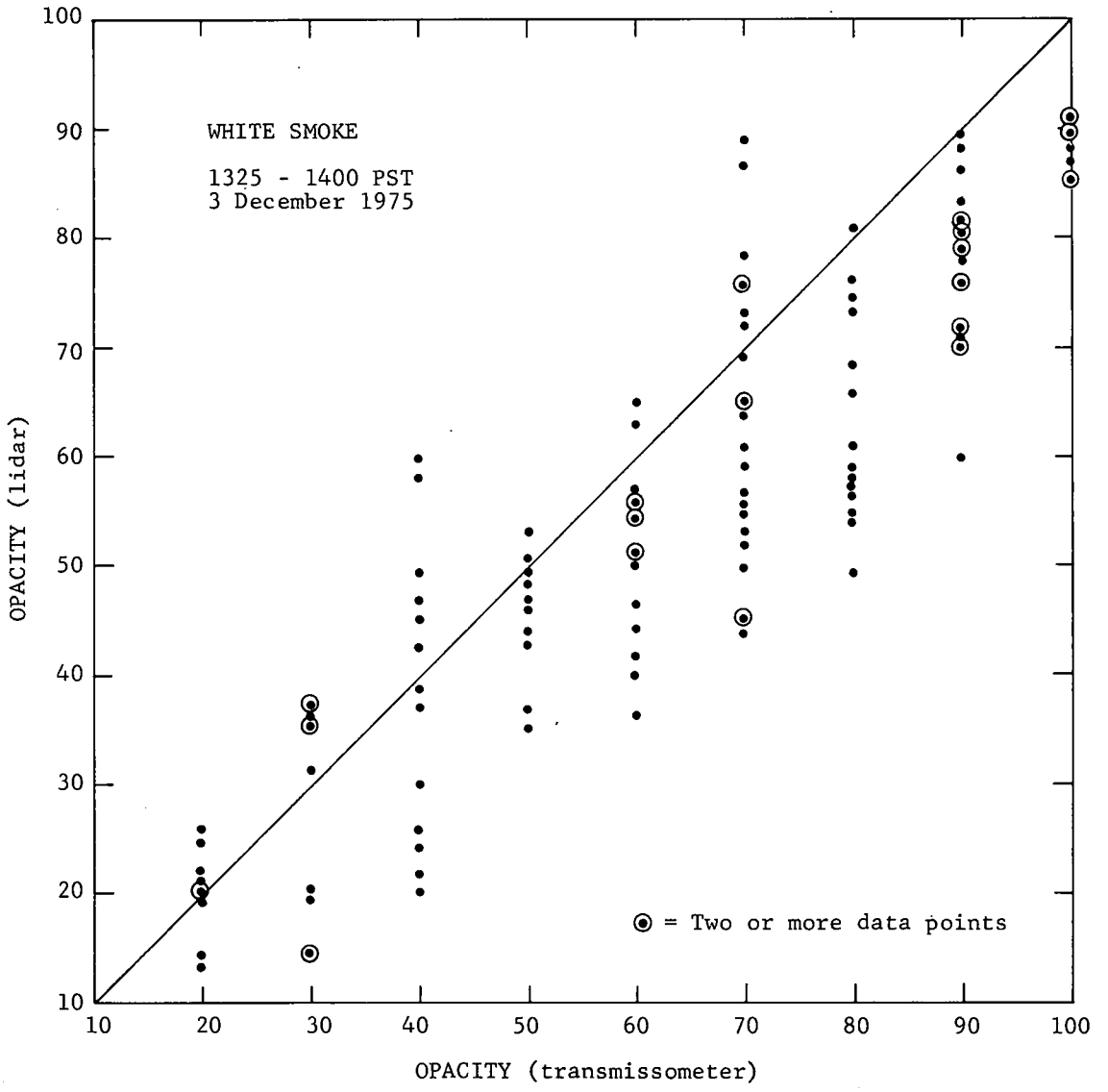

FIGURE 5 OPACITY OF WHITE SMOKE AS MEASURED BY THE LIDAR PLOTTED AGAINST OPACITY FROM TRANSMISSOMETER

clear air in front of the plume, the lidar observed opacity will underestimate the true opacity.

Figure 6 presents the lidar derived opacities plotted against the transmissometer opacities for the data collection period of 1415-1425 PST. These data points show more scatter and more values above the expected 45° line than for the data presented in Figure 5. It was visually noticed that the plume was more "turbulent" in the later data run, and this probably resulted in the lower correlation and greater lidar-observed opacities (especially for the 30, 40, and 50 percent levels) presented in Figure 6.

Figure 7 presents a plot of the plume returns (normalized to the near side clear air returns) against the transmissometer measured opacities for the same data presented in Figure 6. These data also show denser plumes for the 30, 40, and 50 percent opacities than expected from the remaining data.

The plume returns plotted against the lidar-observed opacities are shown in Figure 8. These data clearly show that the lidar derived opacities are consistent with the lidar observed plume densities, and therefore, the lidar opacity technique is considered valid, provided the lidar observes a representative volume of the plume.

The black smoke plumes were more variable in terms of opacity than were the white smoke plumes (see Figure 3). For this reason, the opacities derived from the lidar are not presented here. However, Figure 9 presents the plume returns as a function of lidar-observed opacities for the black smoke that was generated beginning at 1435 PST. It is seen that good correlation is again obtained and that the plume returns are approximately 5 dB (or a factor of 3) less than for white smoke. Therefore, these data well illustrate the sensitivity of the plume backscatter to the absorption properties of the plume particulates.

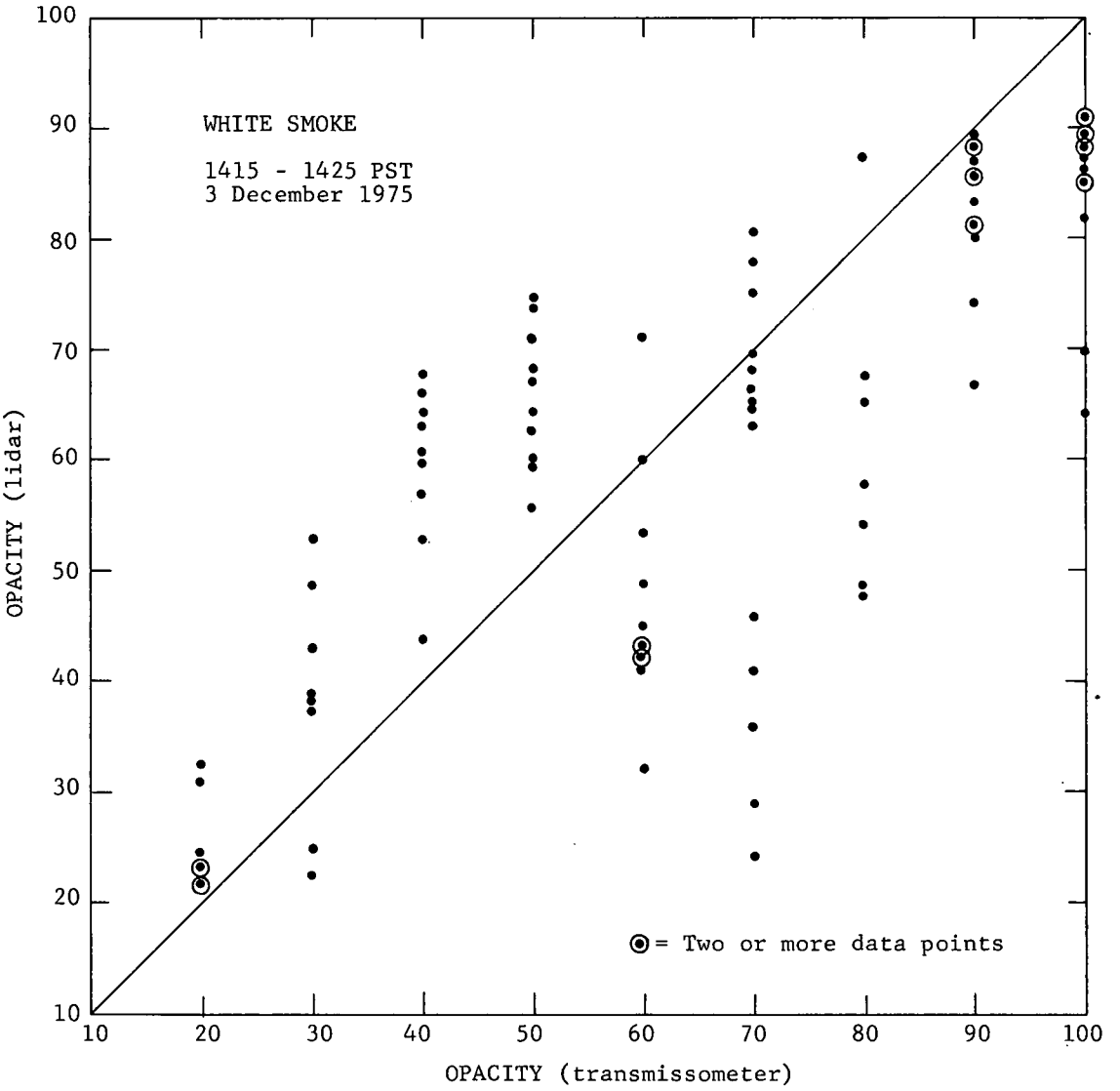

FIGURE 6 OPACITY OF WHITE SMOKE AS MEASURED BY THE LIDAR PLOTTED AGAINST OPACITY FROM THE TRANSMISSOMETER

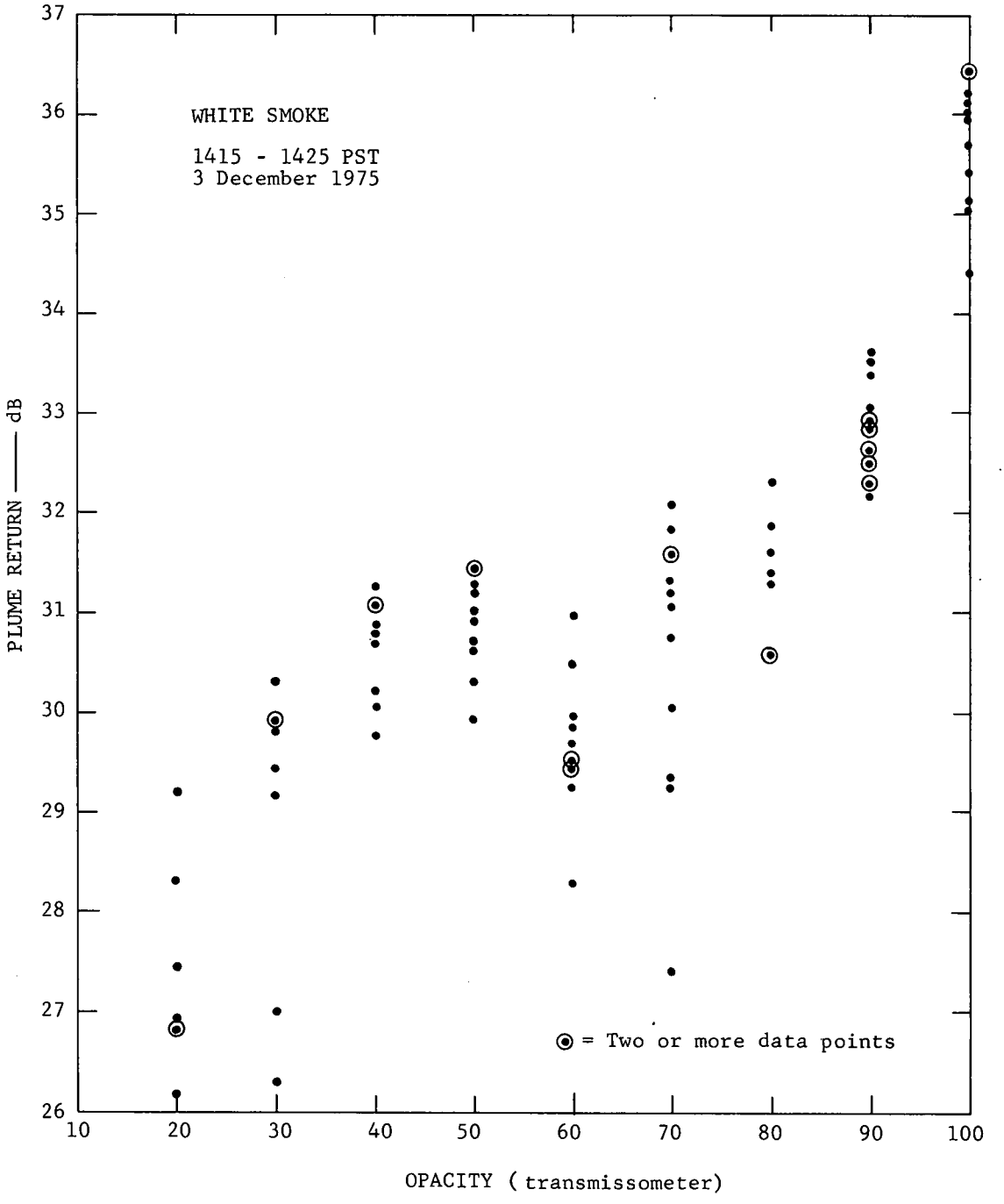

FIGURE 7 LIDAR OBSERVED PLUME RETURNS (normalized to near side clear air returns) PLOTTED AGAINST OPACITY FROM TRANSMISSOMETER

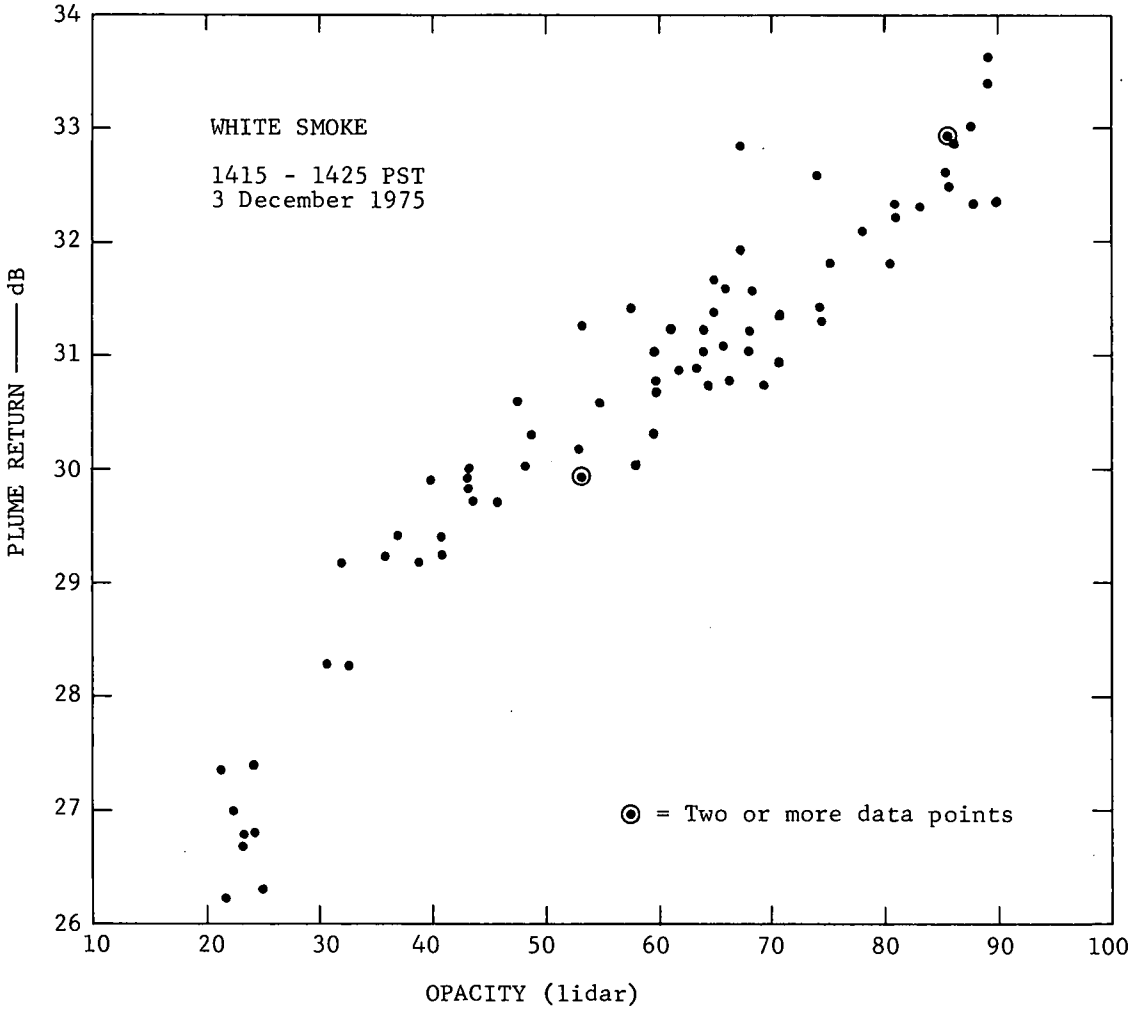

FIGURE 8 PLUME RETURNS PLOTTED AGAINST OPACITIES OBSERVED FROM THE LIDAR (white smoke)

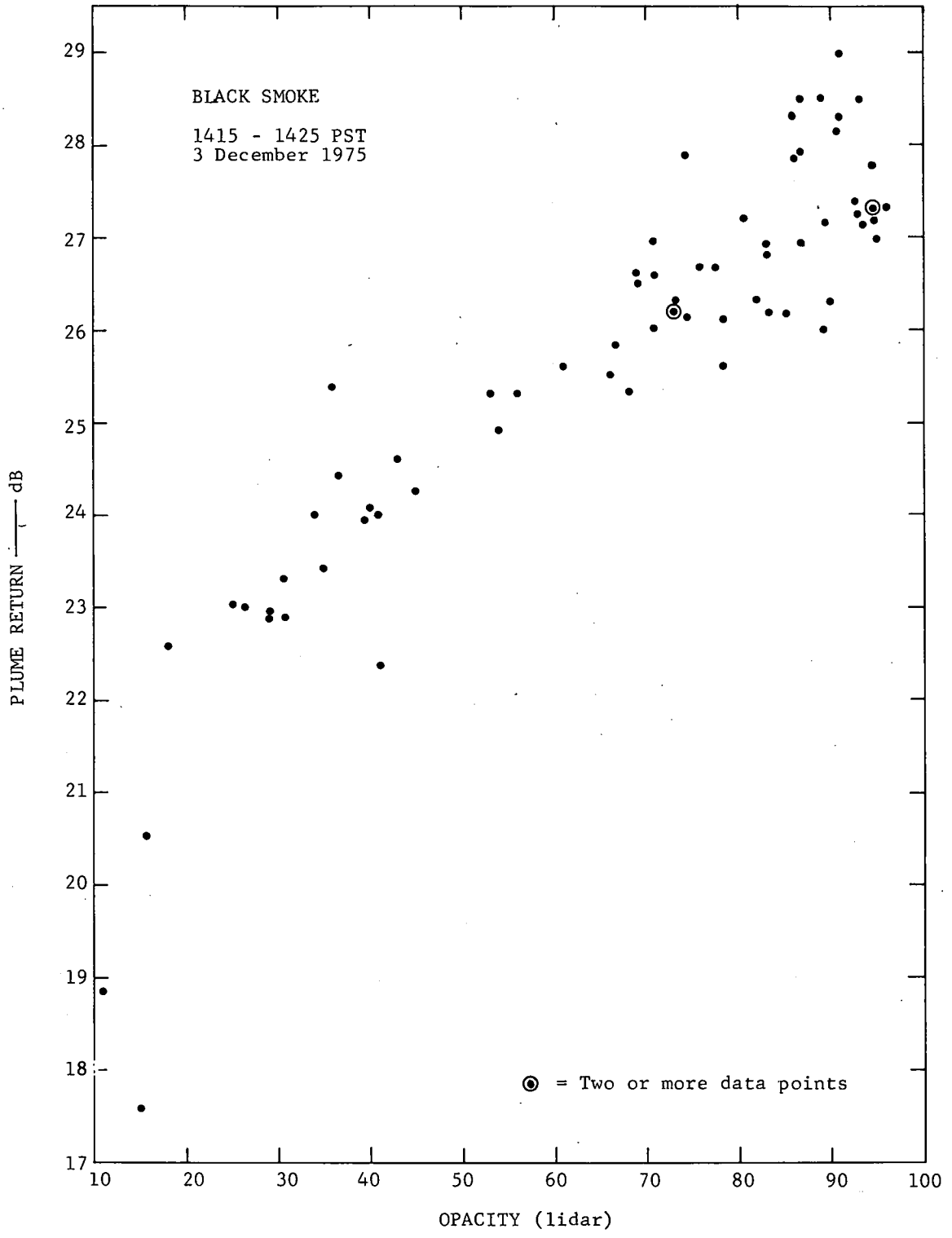

FIGURE 9 PLUME RETURNS PLOTTED AGAINST OPACITIES OBSERVED FROM THE LIDAR (black smoke)

V KAISER-PERMANENTE TESTS

On 2 December 1975 the Mark IX lidar was used to observe stack emissions from the Kaiser-Permanente Cement Company, located in Cupertino, California. These initial observations were confined to testing the suitability of log and linear response receivers and analog range correction. The receiver gain reduction steps were not used. Three plumes were observed--one from a short stack known as Stack 1 and two larger stacks known as West Stack and East Stack. Observations on the East Stack plume gave opacities ranging from 35 to 75 percent with most values near 65 percent. Observations on the West Stack plume gave values of 20 to 75 percent with average values near 50 percent. Stack 1 values were near 20 percent opacity. These opacities are the real-time values computed and printed by the lidar digital system.

Because of possible lidar saturation effects, difficulties in observing the clear air beyond the plume due to a nearby hill, and the limited analysis time devoted to this project, these returns have not been reanalyzed. However, these tests firmly indicated that the log receiver and gain reduction steps were required for plume opacity measurements of dense plumes in low-visibility atmospheres.

In addition to the plume opacity observations with the lidar pointing at a fixed location over the stack, scanning lidar observations were made to derive both vertical and horizontal cross sections of plume structure. The lidar signatures were recorded on DECTAPE with analog range correction applied (see Appendix A). Elevation and azimuth pointing angles were also recorded. The data were then played back through the digital system and displayed on the TV monitor in polar-coordinate form.

Figure 10A presents two elevation scans made sownwind (to the west) of the East and West Stack plumes. The vertical and horizontal scale marks are drawn at spacings of 75 m. The maximum angle of the elevation scans was restricted by the lidar van openings in the direction of observation. These cross sections clearly show the rise of the plumes and their transport towards the lidar van (the van was located on the south side of the plumes). Figure 10B presents two azimuth scans from west (bottom of the picture) to east. These data show the transport and diffusion of the plumes to the west and in the direction of the lidar. Although quantitative estimates of downwind plume densities can be made from these data, this was not attempted in this program.

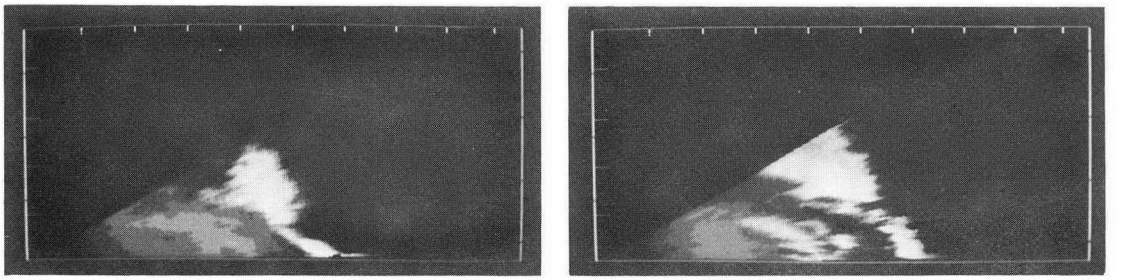

(a) VERTICAL CROSS SECTIONS
(75 m between scale marks)

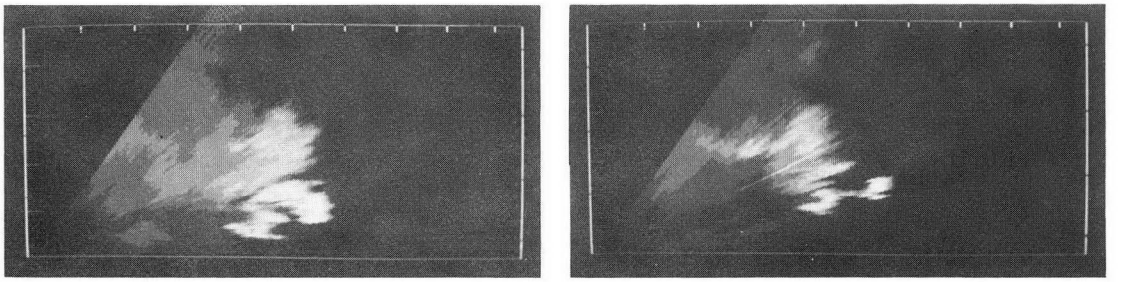

(b) AZIMUTH CROSS SECTIONS
(75 m between scale marks)

FIGURE 10 LIDAR DERIVED VERTICAL (a) AND AZIMUTH (b) CROSS SECTIONS OF PLUME STRUCTURE (2 December 1975; Kaiser-Permanente)

VI OCCIDENTAL AND LIBBY-OWENS-FORD TESTS

Following the smoke generator tests on 3 December, the lidar was used to measure opacities of smoke plumes originating from four stacks (called Stacks 1-4) located within the Occidental and Libby-Owens-Ford manufacturing complexes near Stockton, California. The results are shown in Figure 11. The opacities from Stack 1 varied from 20 to 40 percent with an average around 30 percent. Stack 2 observed opacities were larger and showed more variation (from 40 to 95 percent) than those for Stack 1. Assuming the 40 to 60 percent opacities are a result of the laser beam not adequately positioned on the plume, an average opacity of 80 percent is obtained. The plumes from Stacks 3 and 4 were larger in diameter and, consequently, the lidar beam was more easily positioned so that the full plume was sampled on each lidar firing. The Stack 3 and 4 observations gave average opacities of 90 and 93 percent. These readings were obtained using the log amplifier and gate reduction steps as employed on the smoke generator tests.

Figure 12A presents an azimuth scan (from left to right, but displayed from right to left in the figure) across (and about 5 m above) the top of Stacks 2, 3, and 4 with 150 m between vertical and horizontal scale markings. Figure 12B presents the same data, but with 75 m between scale markings. These data show that Stacks 3 and 4 effectively attenuate the "clear air," causing minimal plume returns from beyond the stack, while this is not the case for Stack 2. This is consistent with the data presented in Figure 11. The transport and diffusion of the stack pollutants downwind are easily visualized from the presentations in Figure 12.

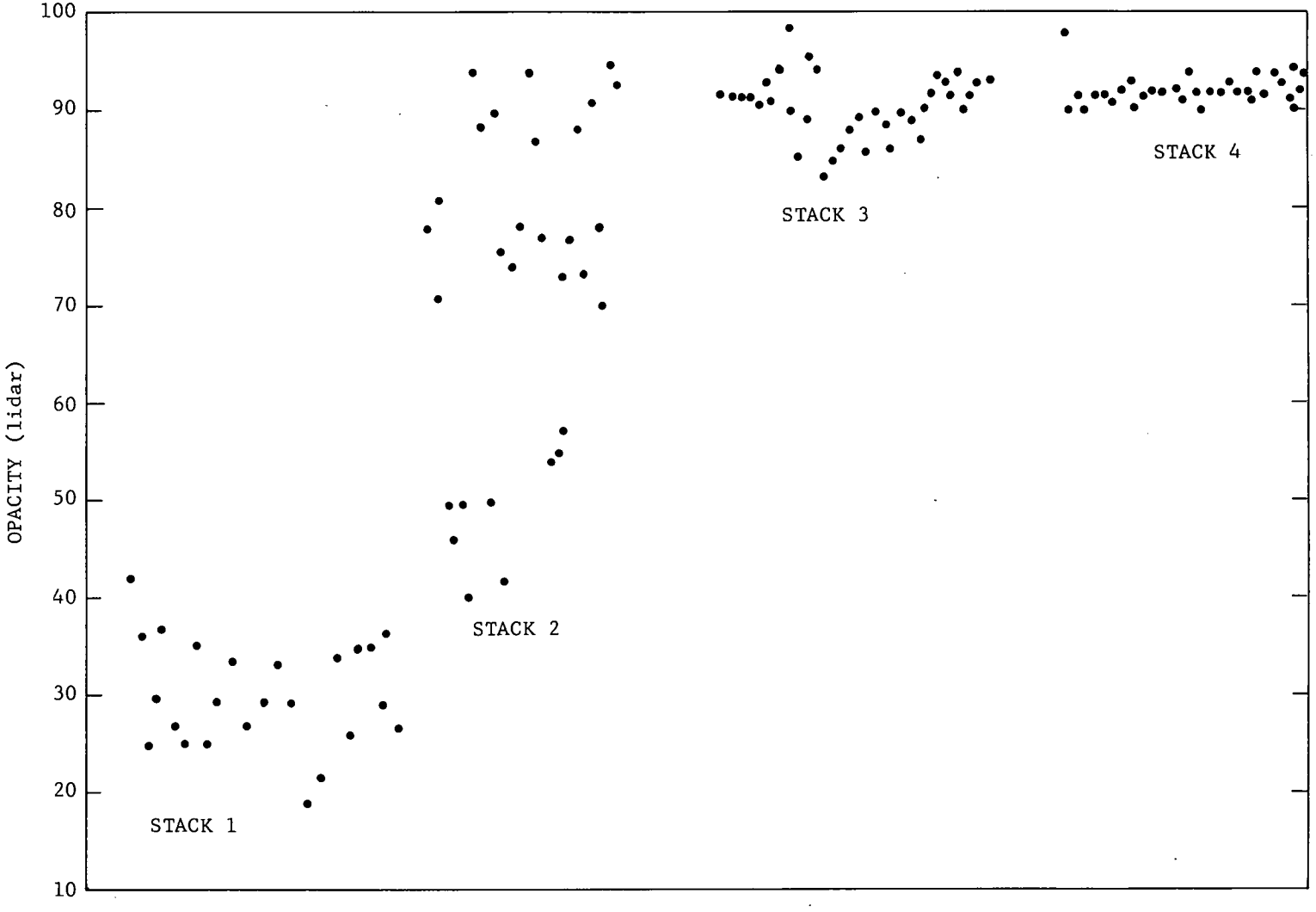

FIGURE 11 LIDAR OBSERVED OPACITIES FOR OCCIDENTIAL (Stack 1) AND LIBBY-OWENS-FORD (Stack 2,3, and 4) PLUMES

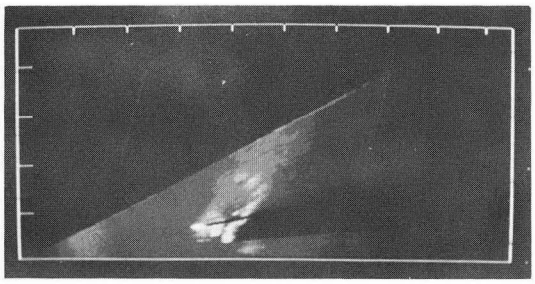

(a) AZIMUTH CROSS SECTION
(150 m between scale marks)

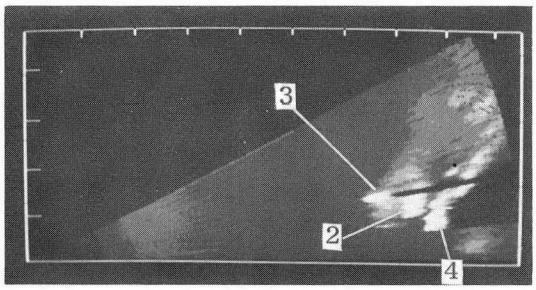

(b) AZIMUTH CROSS SECTION
(plume numbers indicated)
(75 m between scale marks)

FIGURE 12 LIDAR DERIVED AZIMUTH CROSS SECTION OF PLUME STRUCTURE
(3 December 1975; Libby-Owens-Ford)

VII CONCLUSIONS AND RECOMMENDATIONS

This very limited study was conducted to investigate applications of the lidar technique to the remote measurement of opacity of stack emissions and the observation of plume density distributions downwind of the stack. The SRI Mark IX mobile lidar system was used to observe smoke plumes generated from both manufacturing plants and a calibrated smoke source. It was demonstrated that the following specialized features of the Mark IX lidar system greatly aided the plume observations:

- The log amplifier (with nearly 40 dB of dynamic range) allows effective observation of both the clear air and plume particulates.
- The use of receiver gain reduction steps can extend the dynamic range and solves some electronic saturation problems. The two-step gating allows plume opacity measurements in low-visibility atmospheres.
- The advanced capabilities of the digital system permit both real-time and subsequent data processing and display of backscatter information for effective and accurate data collection and analysis.

The results presented in this report demonstrate that the lidar techniques of observing plume opacity (from the near and far side clear air returns) and plume density (from the plume returns) are valid, and can accurately be made with a lidar system such as the SRI Mark IX. The possible difficulties that were evident in this study included:

- Obtaining a representative sample - The shot-to-shot variation in plume opacity and backscatter was primarily a result of plume density variations introduced by the turbulent air flow near the top of the stack. Averaging over many lidar observations would tend to underestimate plume opacity if the beam does

not intercept a representative sample on each firing.

- Clear air inhomogeneities - The "clear" air in low visibility atmospheres (such as near manufacturing complexes) can have large density (backscatter) gradients. Since the opacity measurement requires the assumption of clear air homogeneity in the vicinity of the plume, large errors will result if large inhomogeneities occur.
- Backscatter dependence on particulate properties - The backscatter from a plume is sensitive to particle adsorption (as evident from the results from the white and black smoke observations presented in this report), as well as to particle shapes and sizes. The inference of plume opacity or mass concentration from plume backscatter requires knowledge of the relationships between optical and physical properties and their dependence on particle size, shape, and absorption. Other problems such as multiple scattering and beam defocusing also require consideration.

It is recommended that the evaluation of lidar as applied to plume opacity and density measurement be conducted using a plume of particles with known number concentration sizes, shapes and refractive properties. Only then can experimental accuracies and limitations be properly assessed. The smoke generator used in this study was useful for demonstrating lidar concepts, but is not suited for lidar calibration or research purposes because of the small size of the generated plume.

Figure 13 illustrates a large-scale aerosol chamber designed especially for lidar studies (Uthe and Lapple, 1972). It is suggested that a program to investigate limitations and accuracies of the lidar technique for various optical and physical plume properties could economically be conducted with our existing lidar and aerosol chamber instrumentation.

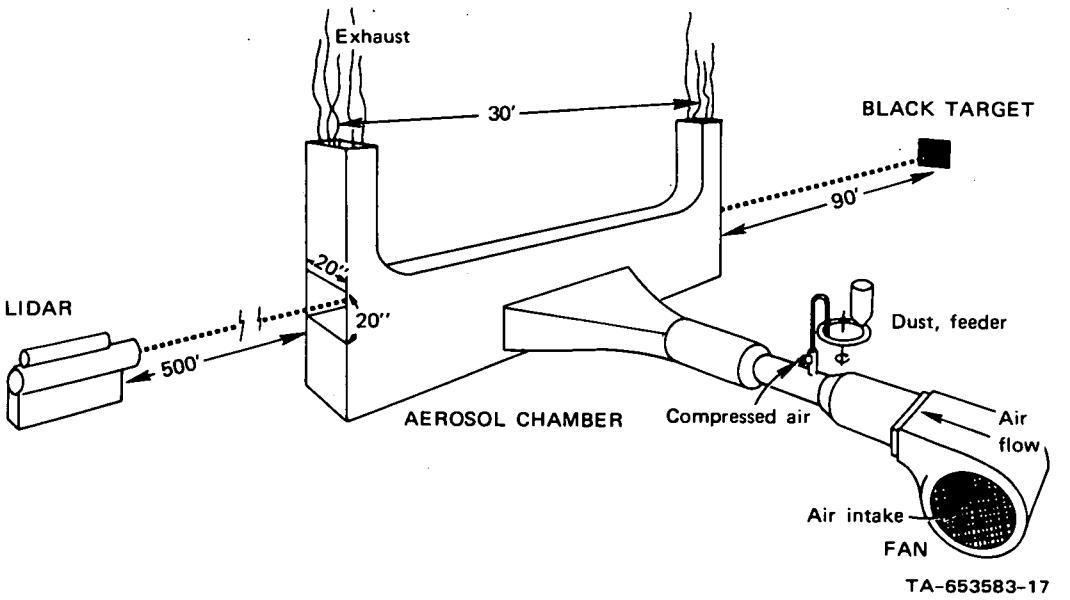

FIGURE 13 DIAGRAM OF EXPERIMENTAL SYSTEM FOR EVALUATING LIDAR TECHNIQUES FOR MEASUREMENT OF PLUME OPACITY AND DENSITY

Appendix A

A DIGITAL REAL-TIME LIDAR DATA RECORDING, PROCESSING AND DISPLAY SYSTEM

Optical and Quantum Electronics 7 (1975) 121–129

Review

A digital real-time lidar data recording, processing and display system*

E. E. UTHE, R. J. ALLEN
Stanford Research Institute, Menlo Park, California, USA

Received 21 November 1974

Application of laser radars to meteorological programs has been limited by the absence of suitable data recording, processing and display techniques. This paper discusses a digital data system that provides the means of performing real-time analysis and display of lidar data. The system is constructed of commercially available components and makes optimum use of available software. Application of the system to the real-time viewing of cirrus cloud structure and inference of cloud density is presented. A review of previously used lidar data handling techniques is also presented.

1. Introduction

Lidar (Light Detection and Ranging) uses laser energy in radar fashion to effectively observe remote atmospheric constituents. Light elastically backscattered from molecules (Rayleigh scattering), suspended particulate matter, and cloud drops and crystals (Mie scattering) can be employed to derive atmospheric structure over extended volumes. In addition, quantitative estimates of atmospheric densities can be made when certain atmospheric conditions exist or when relationships between the optical and physical properties of the scattering medium can be assumed. The Mie scattering technique applied to air pollution measurement has previously been discussed in this journal by Collis and Uthe [1].

The application of Mie scattering lidar techniques to meteorological probing has been limited over the last ten years by a lack of appropriate data recording, processing and display techniques, resulting primarily from the wide bandwidth and large dynamic range requirements of the electronics necessary to process lidar backscatter signatures. Bandwidths greater than 50 MHz are needed to adequately monitor returns from solid reflectors, aerosols and clouds. The amplitude range of the output signal from a lidar photomultiplier tube may extend over more than four decades, but wideband logarithmic amplifiers and gain switching techniques can be used to compress the dynamic range of backscatter signals to be more compatible with data recording and display electronics. In addition to bandwidth and dynamic range problems, the low pulse repetition rates of laser systems have historically limited the application of real-time radar display techniques to lidar data.

The technique used in early lidar systems was to photograph the face of a wide bandwidth oscilloscope where backscatter signal intensity was displayed as a function of range. Fig. 1 presents an example of data collected in this manner during 1969. These particular A-scope displays of lidar backscatter signatures were collected from a downward pointing airborne lidar which was used to investigate properties

*Development of this system was supported by the United States Air Force, Space and Missiles Systems Organization.

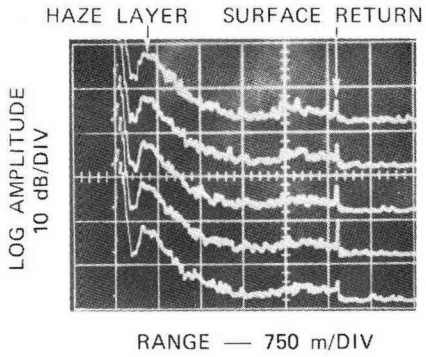

Figure 1 Example of backscatter signatures recorded on Polaroid film in 1969. Data collected from an airborne lidar at an altitude of 3 km and an elevation angle of $-60°$.

of the Sahara dust layer that is transported across the North Atlantic [2]. A video-logarithmic amplifier was used to compress the signal amplitude for recording. Even when multiple traces were recorded on a single photographic print, large amounts of film had to be processed and the meteorologist could not readily interpret the data in terms of atmospheric structure in more than a single dimension. However, with much effort, the photographed backscatter signatures could be hand-processed into presentations depicting time and space contours of backscatter intensity, and these displays of atmospheric structure could be visually inspected for information on atmospheric dynamic, physical and radiative processes. A further step was the digitization of recorded signatures using curve-following techniques, and the computer processing of these digital records into contour maps of backscatter itensity. Fig. 2 presents an example of a computer generated display showing lidar derived structure of the Sahara dust layer. Such presentations are required for effective meteorological use of backscatter lidar techniques.

For certain atmospheric conditions or when appropriate additional information was available, digitized backscatter data could also be

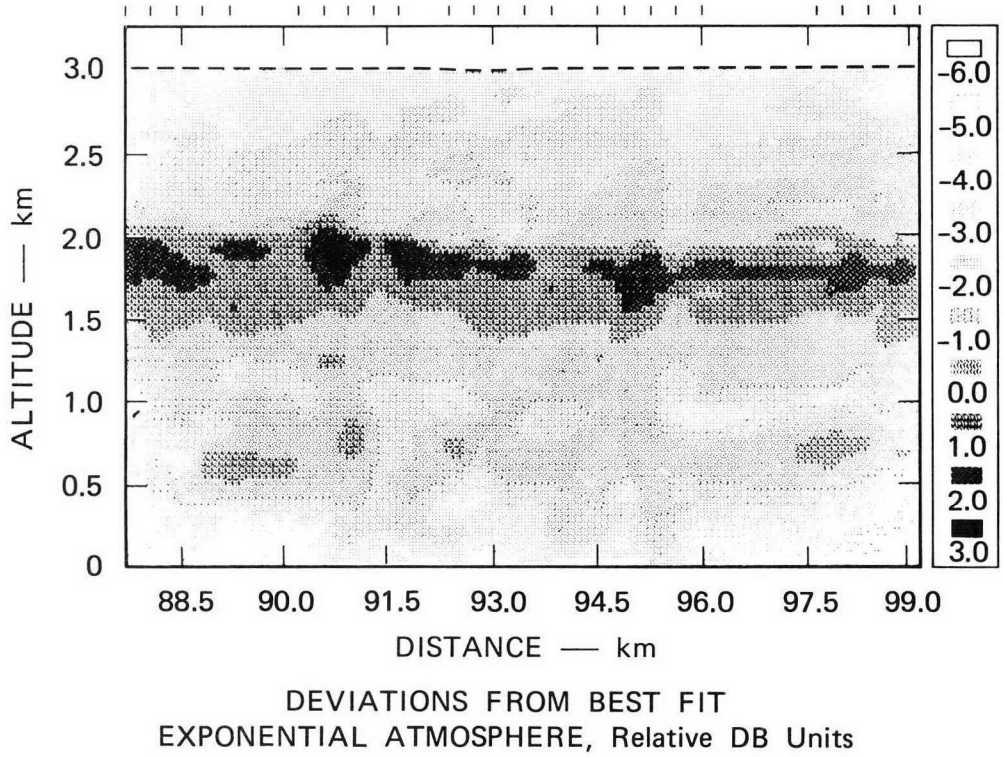

Figure 2 Example of a computer generated cross section of aerosol structure derived from digitized lidar backscatter signatures. Marks above cross section indicate time of laser firing.

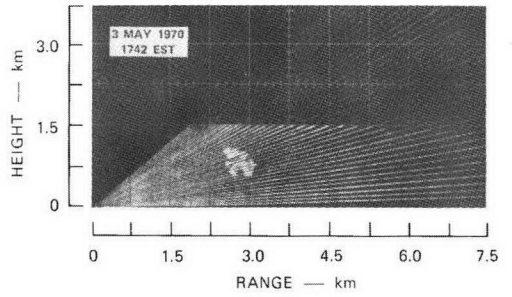

Figure 3 Example of aerosol structure derived from video-disc recording technique. Note the geometry of the smoke plume and haze layer top.

used quantitatively to derive absolute aerosol densities. Although lidar data collection rates were relatively high, the substantial data handling requirements of both the qualitative pattern analysis and the quantitative density analysis typically resulted in the processing of only a small percentage of any collected data set.

A data processing advance was achieved in 1970 when a video disc recording technique was applied to the processing of lidar data for viewing in graphical form [3]. The video disc allowed a format that enabled recorded data to be played back through an electronic system that generated intensity modulated pictorial displays. Fig. 3 presents an example of data processed by the video disc technique [4]. In this example, the lidar was being scanned in elevation in a plane nearly perpendicular to a smoke plume which was rising in a surface haze layer. Each lidar backscatter signature is represented as an intensity modulated line segment with brightness proportional to the logarithm of received signal. In addition to logarithmic amplification, it was necessary to add inverse range squared correction electronics to the photomultiplier detector in order to produce these intensity modulated displays. The video disc system greatly increased the lidar application to real-time and subsequent analysis of time and space variations of atmospheric structure over extended volumes. However, the analog circuitry required to process the data and the 4-MHz bandwidth limitation of the video

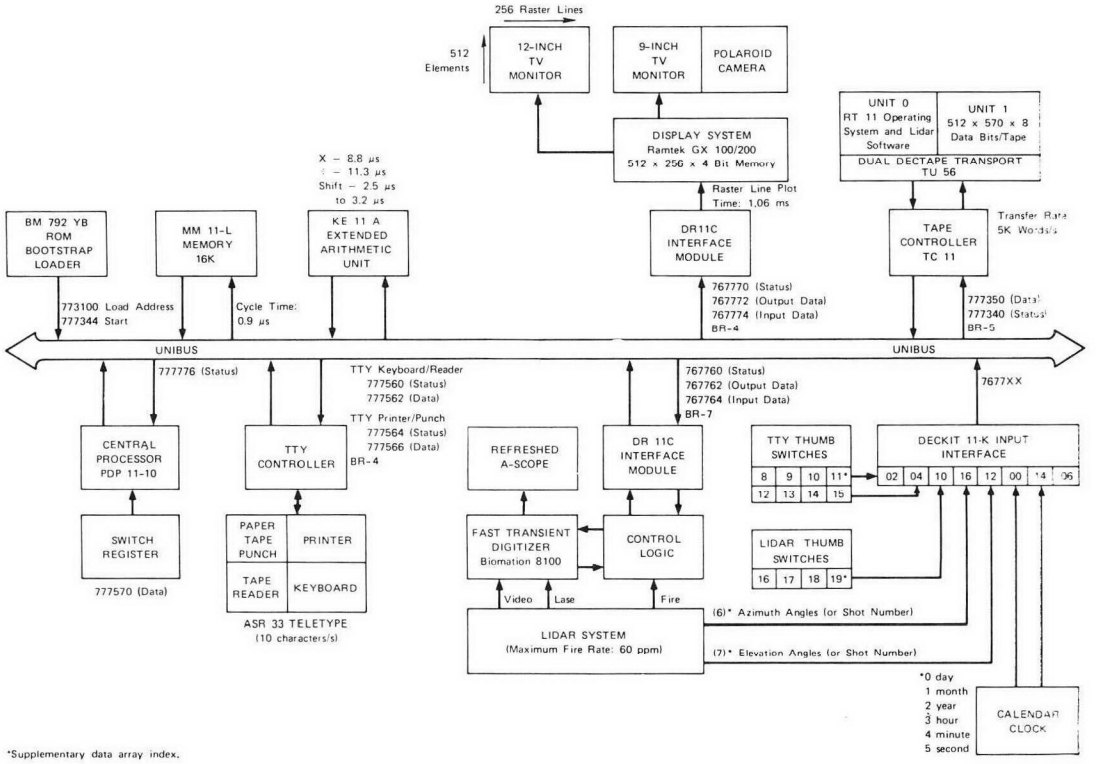

Figure 4 Block diagram of the Mark IX lidar digital system.

disc reduced the data resolution and degraded the quality of the data for quantitative use. For several years, therefore, many lidar programs remained mostly concerned with studies of atmospheric structure rather than absolute aerosol density.

Digital techniques obviously had much to offer in handling lidar data and several groups have, of course, developed systems for this purpose, particularly in upper atmospheric studies where the raw signal is normally in the form of a series of photo-electron pulses. The rapid development of commercial high-speed digitizers and minicomputers now make digital data processing capabilities generally available at relatively low cost; in addition, digital display systems are also available.

This paper describes a digital system constructed from commercially available components that is capable of providing both real-time computer analysis and real-time display of processed lidar data. The system offers all the benefits of digital handling and computation while retaining the very valuable graphical capability shown in the familiar two-dimensional intensity modulated form of Figs. 2 and 3. Large volumes of data may be recorded, processed and displayed in real-time to facilitate operational and research applications.

2. System hardware

2.1. Constraints

Digital data capabilities were added to the existing SRI Mark IX analog lidar system which is installed within a 6 m van complete with its own power generators. About 2000 VA of power and room for one additional 190 cm high cabinet rack were available for the additional equipment.

The Mark IX was constructed primarily for air pollution studies where lidar operation may proceed while the van is moving along urban and rural traffic links. To be compatible, the digital system had to be available to withstand the vibration associated with mobile operation. In addition, new applications required that the new equipment had to withstand hostile environments characterized by high humidity and marine air. This required special considerations for the newly added equipment plus some rework of the existing analog system.

A further constraint was that the design, construction and programming of the digital system was to be completed within a limited funded program that was scheduled to be field operational within a few months.

2.2. Desired Capabilities

The goal was to incorporate a digital system capable of real-time analysis utilizing a versatile interactive gray-scale display system. It was to record all data produced by the lidar, play back the data into the computer for later processing and display, and provide hard copy output summarizing results of quantitative analysis. These capabilities along with the programming requirements are summarized in Table I.

2.3. System description

The digital system that was judged to best meet the desired requirements within the imposed constraints is diagrammed in Fig. 4. It was designed around the UNIBUS concept of the PDP 11 computer system manufactured by Digital Equipment Corporation. The bus physically consists of 56 high-speed (400 ns word transfer) bidirectional and asynchronous communication lines that allow the computer and the peripherals to operate at their maximum speeds. Devices connected to the UNIBUS can send, receive or exchange data without processor intervention and without buffering in memory.

The computer uses 16-bit words but also effectively processes 8-bit data bytes. Eight processor registers allow effective processing of structured word or byte data arrays. A 4-level interrupt system is available for establishing peripheral priority control of the UNIBUS. The bus concept allows a single set of processor instructions to be used for memory reference, operational statements, and input and output of data from peripherals.

The peripherals consist of a Read Only Memory (ROM) for rapid loading of bootstrap instructions, a 16 000 word core memory which can be expanded to 28 000 addressable words, a teletype unit with paper tape read and punch capabilities, and an extended arithmetic unit for hardware integer multiply and divide. The digitizer is the Biomation 8100 that can sample and hold 2000 bytes at sample intervals down to 10 ns. The control logic was designed to allow the lidar rather than the processor to control

TABLE 1 Desired capabilities of the digital system.

Hardware	Real-time analysis	Real-time processing and display, keyboard monitor to control all computer functions of data processing.
	Versatile display	A-scope, Z-scope, alphanumerics, time and height marks, etc.
	Complete recording	$\approx$ 500 data points/trace, azimuth, elevation, time, program control switch data and other data at rates of 60 observations min^{-1}.
	Read capability	Play back of data into computer for later processing and display.
	Hard copy output	Hard copy of results, for real-time operational programs.
Software	Program library	File manipulation, analysis, display, data acquisition, and other programs.
	High level languages	Field operations by scientists and engineers familiar with FORTRAN or BASIC languages.
	Control of branch points and real-time data input	Control type of analysis and input of heights, levels, scales, rates, etc., via data switches, i.e., without stopping program execution.

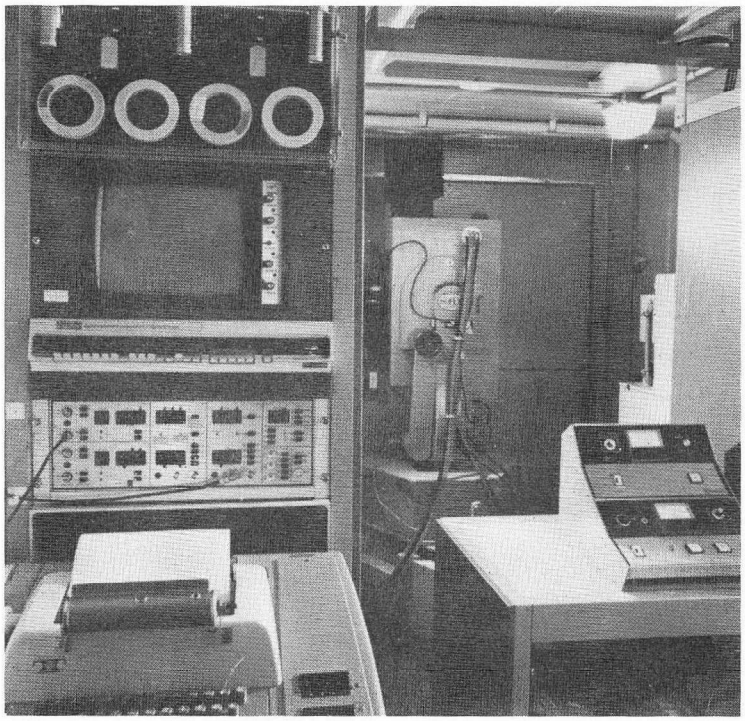

Figure 5 Mark IX digital system. From top to bottom: dual Dectape, TV monitor, PDP-11 minicomputer, Biomation transient digitizer and teletype with sense switches mounted on lower right.

the data collection operation, thereby maintaining the timing required by the analog video disc recording system. In addition to the lidar backscatter data, an input data interface to the bus is used to transfer information to the processor on date, time, azimuth, and elevation

pointing angles of the lidar and manually set switch data for input of supplementary data and program control.

The display system consists of a Ramtek GX200 and a TV screen with vertical raster scans. The Ramtek chosen uses 256 raster scans, each with 512 line elements. Each of the 256 by 512 picture elements displays 4-bit information to generate gray scale pictures consisting of 16 gray steps. This equates to over half a million bits of display memory. Examples of data displays will be presented below.

Magnetic tape was chosen for the recording medium because magnetic discs were judged to be marginal for use during mobile operation of the van-mounted lidar. However, magnetic tape recorders are also vulnerable to humidity, salt spray and vibration. A dual DECTAPE system was selected since it has redundant read/write heads with a medium packing density. The 10 cm diameter DECTAPE reels are preformated into 578 blocks for quasi-random access. One DECTAPE unit is used for data storage with typically 490 8-bit samples per backscatter signature and 22 bytes of supplementary data on each block of tape. The other DECTAPE unit is used as a system device for Digital Equipment Corporation's RT-11 real-time operating system.

Fig. 5 shows the digital system installed within the Mark IX lidar van. The dual DECTAPE unit is on top and has been fitted with a protective plastic cover containing three cylinders each with a desiccant compound and indicator. These were added to reduce the humidity around the heads and magnetic tape. Below the DECTAPE unit is the TV monitor with a 90° rotated yoke for 256 vertical raster lines each with 512 elements of resolution. The PDP-11/10 minicomputer is next with the Biomation 8100 shown below the computer.

3. System software

The RT-11 real-time operating software available from the computer manufacturer includes a keyboard monitor, peripheral interchange package, and various operational programs such as an assembler, a BASIC language interpreter, and a FORTRAN compiler.

The basic data handling programs are written in assembly language and are linked with the higher level language packages. These routines

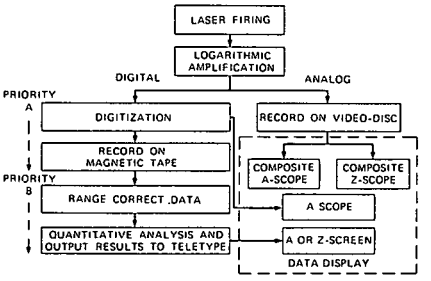

Figure 6 Flow diagram of lidar signature processing and display.

are callable from FORTRAN or BASIC data acquisition and analysis programs. The user and service programs reside on DECTAPE to allow rapid building of a program library of nearly unlimited size.

Fig. 6 illustrates the data flow for each lidar firing. After logarithmic amplification, the signal is routed to both the analog and digital processing units. The digitizer control functions may be set or adjusted either by the operator or the computer program that is under execution. Between lidar firings, 2000 data bytes are retained by the internal digitizer memory that continually refreshes an oscilloscope display of signal amplitude as a function of range. This display provides the operator a real-time view of the latest backscatter trace and also an indication of digitizer performance. A specified number of data bytes (typically 490) are transferred to core memory and are immediately written on magnetic tape along with 22 bytes of housekeeping data as Priority A. Upon completion of Priority A operations, the digital system performs a set of operations designated as Priority B. These operations are interrupted at any time the lidar is fired in order to perform the Priority A operations for the data resulting from the lidar firing. Upon completion of Priority A operations, the control of the digital system reverts back to the processing of Priority B operations at the point of interruption. This procedure allows real-time recording of all data and further processing of a percentage of the data determined by the length of the Priority B operations and the lidar fire rate. At a later time, the recorded data can be played back with the Priority B operations performed on all collected data. Priority B operations are normally directed

to the display of lidar data and inference of aerosol or cloud densities.

4. Examples of system applications

The capability of the digital lidar system can be illustrated by the following examples of how it is used to monitor cirrus cloud structure and densities in real-time. The Priority B operations include:

(1) Correction of the lidar trace for the inverse range-squared dependence and instrument response functions;
(2) computation of cloud densities over an altitude interval determined by input switch data. The computation assumes a clear air density at the lower input altitude, a mean crystal radius, and a factor between the backscatter and extinction coefficients that includes a multiple scattering correction [5]. An approximate correction for cloud attenuation is made on the basis of observed cloud thickness and relative density as determined by the maximum cloud-to-clear air ratio;
(3) output of the computational results to the teletype;
(4) plot of the complete lidar signature on the digital screen.

These operations could be performed on the data resulting from each lidar firing with a lidar fire rate of 6 min^{-1} and a density computation on over 100 data points i.e., for a cloud 3 km thick.

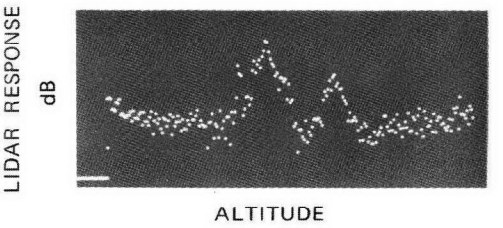

Figure 7 Example of a digital A-screen plot showing two cirrus cloud layers.

The choice of Z-screen or A-screen and the plot scaling factors (dB/gray step or dB/line element) are specified by the sense switch settings which are sampled for each lidar firing. The plot data are referenced to the minimum digitizer value (−128 counts) at a range of 9 km. In addition to the display of lidar data, a sense switch option allows the painting of a 16-gray scale step function on the display screen. This is useful for real-time evaluation of cloud densities and for adjusting the screen brightness and contrast controls for viewing and photographing the complete 16-gray step levels. Examples of digital output are presented below.

Fig. 7 shows an A-screen presentation plotted across the screen using every other point of the 490 data point array. This particular data

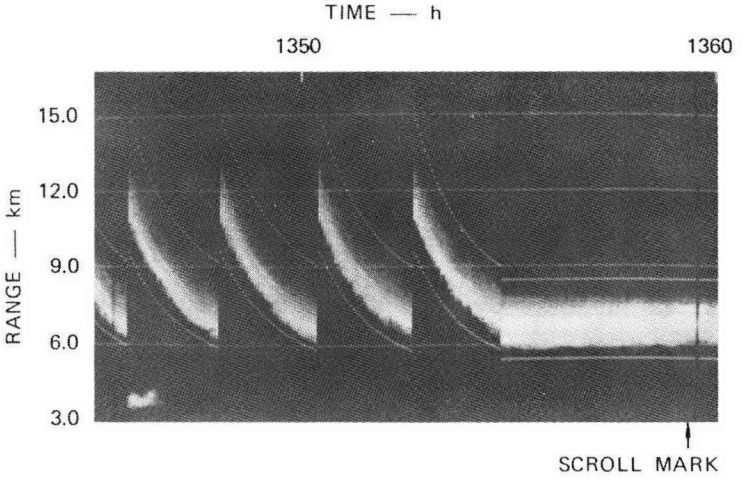

Figure 8 Example of a digital Z-screen plot showing structure of a 6-8 km cirrus layer. Curved lines and data indicate that the lidar was being scanned in elevation during the data collection.

TABLE II Examples of lidar digital data output.

H	Min	S	Height	Density	Number	Liquid water	Column content
14	0	11	6.735	28.6438	48989.1	1.47748	2.92177
14	0	14	6.735	26.8712	32571.7	.982341	2.09537
14	0	17	6.735	27.7394	39779.7	1.19973	2.30663
14	0	20	6.735	27.7756	40112.4	1.20976	2.47013
14	0	23	6.735	28.7885	50648.9	1.52754	3.26136
14	0	26	6.765	28.3339	45476.3	1.37154	3.01024
14	0	29	6.735	27.4862	37526.5	1.13178	2.50087
14	0	32	6.735	26.7627	31767.8	.958098	2.05492
14	0	35	6.735	27.5224	37840.4	1.14124	2.41707
14	0	38	6.765	28.0445	42544.6	1.28312	2.34013
14	0	41	6.735	29.6929	62374.8	1.88118	3.79786
14	0	44	6.765	27.5019	37547.5	1.13241	2.21339

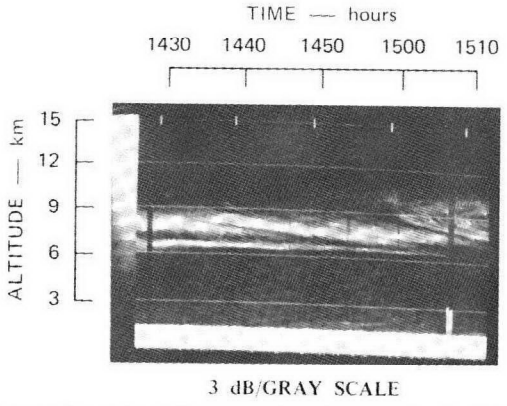

Figure 9 Example of Z-screen plot of 16-gray scale steps and of a cirrus layer that is non-uniform in structure and density.

illustrates the range corrected backscatter signal from multiple cirrus layers. The detector has been gated off for the first 1.5 km to prevent electronic saturation by low-altitude boundary layer clouds. Thus far we have not made extensive use of A-screen plots and have not yet added vertical and horizontal scale markings.

Fig. 8 shows an example of a gray scale Z-screen plot. Initially the lidar was being scanned in elevation angle, and the curved lines represent the height limits of integration as input by the operator, in this case, from 5.5 to 8.5 km. Time marks are determined from the digital clock and in this case are spaced at 10 min intervals. The black raster line indicates the end of a 256 line plot and the screen has begun to scroll left erasing the first raster line and adding the last line for each lidar firing so that the last 256 lidar signatures are always displayed.

Table II presents an example of the teletype output. The first columns list the times of lidar firings. In this case the lidar was being fired every 3 s. In real-time, the cloud density analysis was completed for every second lidar firing. The next columns give the height of maximum cloud density in km, the cloud-to-clear air density ratio in dB, the inferred crystal concentration in crystals per m^3 and ice water content in g m^{-1} at the height of maximum cloud density, and the last column gives a quantity related to the vertically integrated liquid water content.

Fig. 9 presents a Z-screen with the 16 bright-

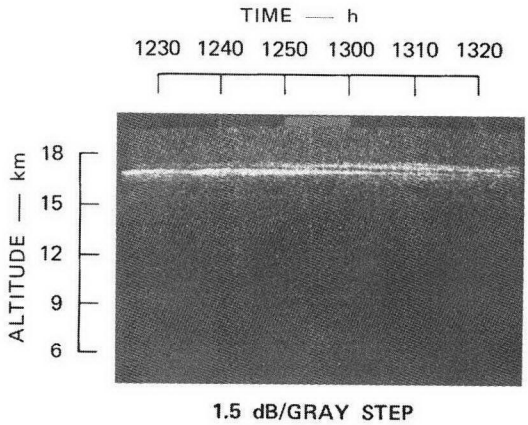

Figure 10 Z-screen plot of a high-altitude low density cirrus cloud.

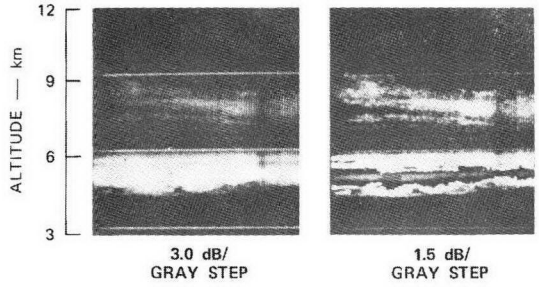

Figure 11 Example of digital iso-contouring applied to the presence of a high- and low-density cirrus cloud.

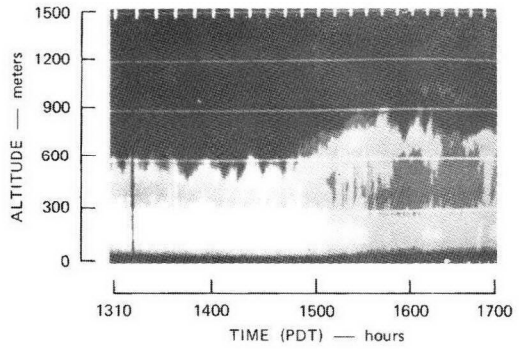

Figure 12 Example of a digital Z-screen presentation of the low altitude pollution layer over Menlo Park, California, 22 October 1974.

ness levels plotted on the left-hand side of the screen. In this case, the operator used 3 dB per gray step. The lower area represents a range interval for which the detector was gated off. The difficulty of photographically reproducing a TV screen presentation is shown by this figure. The curved lines and reduction of gray steps were introduced by the photography. A corresponding loss of cloud structure as compared with that observed on the actual screen occurs in all the presentations here.

Fig. 10 illustrates the Z-screen presentation for a low-density (2×10^{-4} g m^{-3}) high-altitude cloud.

Fig. 11 illustrates the iso-contouring capability of the Mark IX digital system. When the maximum brightness scale is exceeded, the data is recirculated to the low brightness gray steps. In this manner, a low dB/gray step factor may be used to give good visual display of low-density clouds while still getting a dB reading on high-density clouds.

Fig. 12 presents a Z-screen example of the structure of the lower atmospheric pollution layer observed over Menlo Park, California. The new digital capabilities of the Mark IX lidar should greatly increase the possibility of relating screen brightness to aerosol density for lidar studies of the pollution layer [6]. It is planned to investigate applications of the digital system in connection with other remote sensing instrumentation, such as backscatter acoustic sounder and radio-acoustic sounding systems.

5. Conclusion

In conclusion, a relatively low-cost lidar data recording, processing and display system, possessing many capabilities required for efficient meteorological operation of lidar, has been constructed and demonstrated.

References

1. R. T. H. COLLIS and E. E. UTHE, *Opto-electronics* **4** (1972) 87-99.
2. E. E. UTHE and W. B. JOHNSON, Lidar observations of the lower tropospheric aerosol structure during BOMEX, Final Report, SRI Project 7929, AEC contract AT(04-3)-115 (1971).
3. R. J. ALLEN and W. E. EVANS, *The Review of Scientific Instruments* **43** (1972) 1422-32.
4. W. B. JOHNSON, 'Lidar Measurements of plume diffusion and aerosol structure,' paper presented at the American Meteorological Society Conference on Air Pollution Meteorology, Raleigh, North Carolina, USA (April 1971).
5. C. M. R. PLATT, *Journal of Atmospheric Sciences* **30** (1973) 1191-204.
6. E. E. UTHE and P. B. RUSSELL, *Bulletin of the American Meteorological Society* **55** (1974) 115-21.

REFERENCES

Allen, R.J., and W.E. Evans, 1972: Laser radar (LIDAR) for mapping aerosol structure. Rev. of Sci. Inst., 43, 1422-1432.

Cook, C.S., G.W. Bethke, and W.D. Conner, 1972: Remote measurement of smoke plume transmittance using lidar. Applied Optics, 11, 1742-1748.

Evans, W.E., 1967: Development of lidar stack effluent opacity measuring system. Phase I and Ia Reports--Design Studies, Edison Electric Institute, SRI Project 6529. Stanford Research Institute, Menlo Park, California.

Fernald, F.G., and R.T.H. Collis, 1965: Report on experiments to explore the feasibility of measuring the opacity of stack effluents by lidar. Report submitted to Edison Electric Institute, SRI Project 5564. Stanford Research Institute, Menlo Park, California.

Johnson, W.B., 1969: Lidar observations of the diffusion and rise of stack plumes. J. Applied Meteorology, 8, 443-449.

Johnson, W.B., R.J. Allen, and W.E. Evans, 1973: Lidar studies of stack plumes in rural and urban environments. Final Report Contract CPA 70-49, Environmental Protection Agency, SRI Project 8509. Stanford Research Institute, Menlo Park, California.

Johnson, W.B., and E.E. Uthe, 1971: Lidar study of the Keystone stack plume. Atmos. Environ., 5, 703-724.

Uthe, E.E., and R.J. Allen, 1975: A digital real-time lidar data recording, processing, and display system. J. Optical and Quantum Electronics, 7, 121-129.

Uthe, E.E., and C.E. Lapple, 1972: Study of laser backscatter by particulates in stack emissions, Final Report Contract CPA70-173, Environmental Protection Agency, SRI Project 8730. Stanford Research Institute, Menlo Park, California.

GPO 833-343